NASA CONTRACTOR REPORT

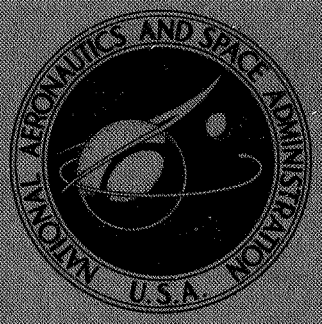

NASA CR-1305

NASA CR-1305

HYDROGEN GAS PRESSURE VESSEL PROBLEMS IN THE M-1 FACILITIES

by J. S. Laws, V. Frick, and J. McConnell

Prepared by
AEROJET-GENERAL CORPORATION
Sacramento, Calif.
for Lewis Research Center

NATIONAL AERONAUTICS AND SPACE ADMINISTRATION • WASHINGTON, D. C. • MARCH 1969

NASA CR-1305

HYDROGEN GAS PRESSURE VESSEL PROBLEMS IN THE M-1 FACILITIES

By J. S. Laws, V. Frick, and J. McConnell

Prepared under Contract No. 3-2555 by
AEROJET-GENERAL CORPORATION
Sacramento, Calif.

for Lewis Research Center

NATIONAL AERONAUTICS AND SPACE ADMINISTRATION

For sale by the Clearinghouse for Federal Scientific and Technical Information
Springfield, Virginia 22151 – CFSTI price $3.00

ABSTRACT

This report delineates pertinent data and information related to a series of failures, or structural defects, experienced with high pressure, gaseous hydrogen storage receivers procured for, installed, and used as part of the M-1 Engine Development Program.

FOREWORD

The research described herein was conducted by the Aerojet-General Corporation, Liquid Rocket Operations. It was performed under NASA Contract NAS 3-2555 with Mr. W. H. Rowe, Airbreathing Engines Division, NASA Lewis Research Center, as Technical Manager. The report was originally issued as Aerojet-General Report No. 8800-67, April 1966.

TABLE OF CONTENTS

TABLE OF CONTENTS (Cont.)

LIST OF TABLES

LIST OF FIGURES

LIST OF FIGURES (Cont.)

LIST OF FIGURES (Cont.)

I. SUMMARY

This report presents pertinent data and information related to a series of structural defect failures experienced with high-pressure, gaseous hydrogen storage receivers that were procured by the Aerojet-General Corporation for the M-1 Engine Development Program at its Sacramento Facility.

The gas receivers involved are multilayer, 1300 cu ft (water volume) 5000 psi units, which are manufactured of high-strength carbon steel by the A. O. Smith Corporation and the Struthers-Wells Corporation. These receivers (60-in. inside diameter and 70 ft long) incorporate monoblock hemispherical heads and each receiver has a centered eight-inch main discharge nozzle. The multilayer, cylindrical body contains three, widely-spaced one-inch (or one-inch and two-inch in the case of the Struthers-Wells Corporation) inside diameter accessory nozzles for drain, recharge, relief, or vent connections.

Three of the four installed A. O. Smith receivers failed structurally at a one-inch accessory nozzle location; this represented three of the total ten nozzles. These failures consisted of a crack, or cracks, through the nozzle forging that admitted gas around the inner, gas-tight lamination and into the vented layers. One unit failed twice at the same nozzle location after the nozzle had been completely replaced between failures. A large crack was detected in the weld metal surrounding the main eight-inch discharge nozzle of another unit which was under repair for a one-inch nozzle failure.

The results of exhaustive metallurgical and other investigations concerning the third A. O. Smith receiver (VH-74) failure are presented herein. A digest of the literature and an industry survey for causative factors also are discussed. Investigations included metallurgical laboratory analysis of cracked nozzle specimens, stress analysis of the failure area, and a review of all recently-recorded research and laboratory investigations into the affect of gaseous hydrogen upon metal properties. In addition, leading government and industry metallurgical consultants were interviewed.

The following six failure modes were considered and investigated:

- Non-specification materials.
- Stress corrosion.
- High or low cycle fatigue.
- Low temperature embrittlement.
- Excessive stresses.
- Hydrogen embrittlement caused by low temperature, high-pressure gas.

Conclusions concerning the A. O. Smith receivers and recommendations for corrective and preventative actions are presented.

A single Struthers-Wells receiver, which was fabricated with four layers of T-1 steel, failed after only a few days of service. Subsequent detailed examination, including destructive disassembly, established that there had been inadequacies during the manufacturing. Preliminary inspection of two other new, unexposed Struthers-Wells receivers revealed cracks in the inner layer.

II. INTRODUCTION

The design of new hydrogen test facilities for installation in H-Zone of the Liquid Rocket Operations Test Area was initiated in 1961. It included a cascade of four 1300 cu ft receivers to provide stored, 5000 psi hydrogen gas for pressurization of liquid hydrogen run vessels, for injection and mixing with liquid hydrogen for uncooled chamber testing, and for gas purges. The second increment of two receivers was funded and procured by the M-1 Program, Contract NAS7-141(F). The combined installation is shown on Figure No. 1.

The gaseous hydrogen storage system was designed for 5000 psi maximum operating pressure. The receivers were designed and fabricated in conformance with the Industrial Safety Orders, Unfired Pressure Vessel Code, of the State of California, which is primarily based upon Section 8 of the ASME Unfired Pressure Vessel Code.

The design point of 5000 psi was selected for three reasons: the economics of storage receivers (low dollar/cu ft unit cost); this pressure represented the current upper limit for proven cryogenic pump-vaporizer equipment; and 5000 psi provided adequate flow and control pressure differential for propellant run-vessel pressurization.

The procurement specifications utilized were extensions of, and refinements to, previously successful specifications for smaller, lower-pressure equipment.

Vessel material compatibility with the stored gas was required by M-1 Specification 6289. However, the material of construction was not specified.

Receivers under parallel procurement for gaseous nitrogen application were fabricated as nearly identical as possible to the hydrogen units.

Detailed stress design, welding design and practices, as well as the selection of materials were controlled by applying the standards of the California Code and the ASME Unfired Pressure Vessel Code.

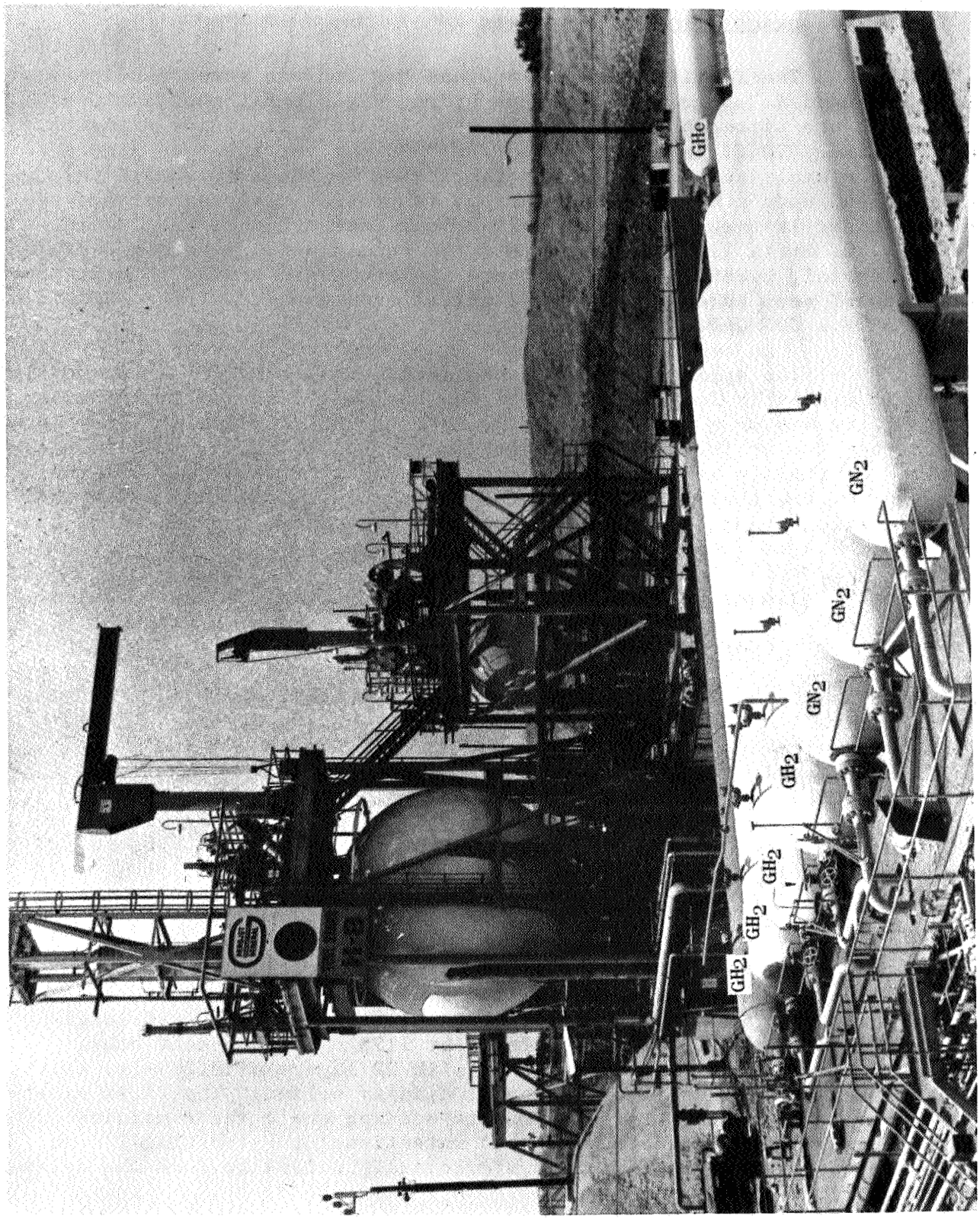

Figure 1
Receiver Installation, H-Area

III. TECHNICAL DISCUSSION - A. O. SMITH RECEIVERS

A. DESCRIPTION OF RECEIVERS

The facilities at Test Stand H-8 include seven receivers; four are used to store high-pressure hydrogen gas and three to store high-pressure nitrogen gas. All the vessels are 5 ft inside diameter, approximately 70 ft long, and rated for 5000 psi service (see Figure No. 2). The vessels were designed and fabricated by the A. O. Smith Corporation based upon a multilayer principle to provide compressive stresses on the inner layers. The inner cylindrical pressure shell is 1/2-in.-thick A. O. Smith 1146a material, and the remaining 22 layers are of the same material, 0.289-in.-thick. These 22 layers are vented to atmosphere by means of weep holes. The hemispherical ends are made from 4-3/8-in. thick ASTM A 225 GRB.

The openings in the tanks include an 8-in. gas inlet nozzle, which is centrally located in one of the hemispherical heads, and either a 16-in. manway or a 4-in. nozzle in the other head. In addition, there are either two or three 1-in. nozzles in the vessel walls. One is located at the top and one at the bottom, approximately 7 ft from the junction of the shell and head containing the 8-in. inlet nozzle. The third nozzle, when used, is on the top of the vessel, approximately 54 ft from the same junction.

Vessel VH-74 materials and weld rods are tabulated below:

Component	Material
Pressure Shell	A. O. S. 1146a
Outer Layers	A. O. S. 1146a
Hemispherical Heads	ASTM A 225 GRB
Eight-Inch Nozzle	ASTM 105 GR2
One-Inch Nozzle	A. O. S. 5002 Mod.
Pressure Shell Longitudinal Weld	SW-35, CO-87 Wire, Linde 80 Flux
Shell Girth Welds	SW-120A
One-Inch Nozzle Weld	SW-120A
Head Nozzle Weld	SW-47

The vessel fabrication consists of rolling and welding 1/2-in. thick, 8 ft wide plate into 5 ft diameter x 16 ft cylindrical sections which are joined by a circumferential weld and staggered longitudinal welds that are stress-relieved at 1175°F for one-half hour. These 16 ft sections are then wrapped with 22 layers of 0.289-in. thick, 16 ft wide sheet; each layer is longitudinally welded. The first nine layers are tension prestressed prior to welding while the remaining layers are wrapped and welded without intentional prestressing. Four such 16 ft subassemblies are circumferentially welded to form the cylindrical portion of the vessel.

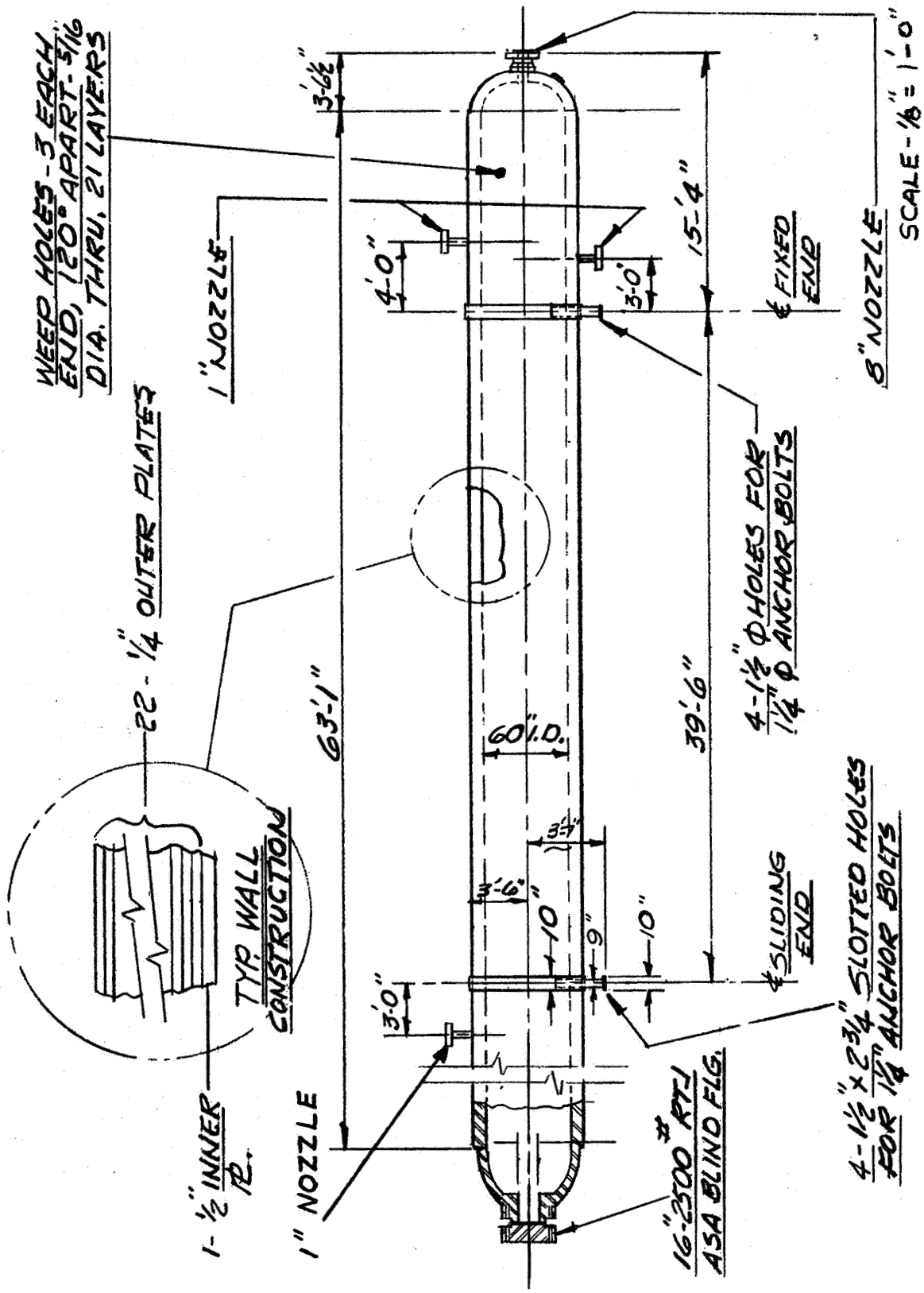

Figure 2

Gaseous Hydrogen High-Pressure Receivers

The 1-in. inside diameter x 2-1/4-in. outside diameter nozzles are inserted through a 4-1/4-in. diameter hole machined through the 23 layers which make up the vessel shell (see Figure No. 3). The joint design consists of a 1-in. wide, straight-sided circumferential joint around the nozzle. The joint is manually-welded from the inside of the vessel with a SW 120A electrode. No stress relief is applied to this weld. The 8-in. and 4-in., or 16-in. manways are manually-welded into the hemispherical heads and stress-relieved at 1150°F for four and three-quarter hours. Then, the heads are welded to the cylindrical shell to complete the assembly. The tanks are required to pass a 7500 psi hydrostatic proof test.

B. HISTORY OF FAILURES

The tanks received from A. O. Smith Corp. were placed in service between September 1963 and July 1964. Since that time, three of the vessels placed in hydrogen service have developed a total of four leaks (see Figure No. 4). All of these leaks have been in the 1-in. nozzle or the associated weldment, located near the discharge end of the vessel. A crack also was detected in an 8-in. nozzle weld in a hemispherical head. This crack did not penetrate the entire weld nor did it cause tank leakage.

Table 1 is a listing of the failures as well as a service history of the vessels. The first leak in vessel VH-3 and the leak from VH-73 were reported to have been from a radial crack in the 1-in. nozzle material. In both cases, the nozzle material was drilled out and replaced by a new nozzle. During the process of repairing the nozzle on VH-73, a crack was discovered in the 8-in. nozzle-to-head weld. This crack was restricted entirely to the weld, covered an arc of 60-degrees, and extended up to one-half of the weld depth. The crack was ground out and repaired. Approximately seven months after the repair of the 1-in. VH-3 nozzle, the vessel developed a second leak in the repaired nozzle. This leak resulted from a crack in the repaired circumferential weld. Again, the crack was repaired and the vessel returned to service. All repaired vessels were hydrostatically proof tested to 7500 psi prior to reinstatement into service.

The latest leak occurred on 11 January 1965 in vessel VH-74 after approximately five months of service. This vessel was pressurized to 4600 psi with gaseous hydrogen and had been holding the pressure for 72 hours prior to failure. Again, the leak was associated with the 1-in. nozzle. When this failure occurred, the Test Division requested assistance from Liquid Rocket Operations Materials Engineering to determine the possible cause of the vessel failures. This report presents the failure analysis investigation conducted on a portion of the failed nozzle and weld. The remaining portion of the nozzle and weld was submitted to the A. O. Smith Corp. for an independent analysis.

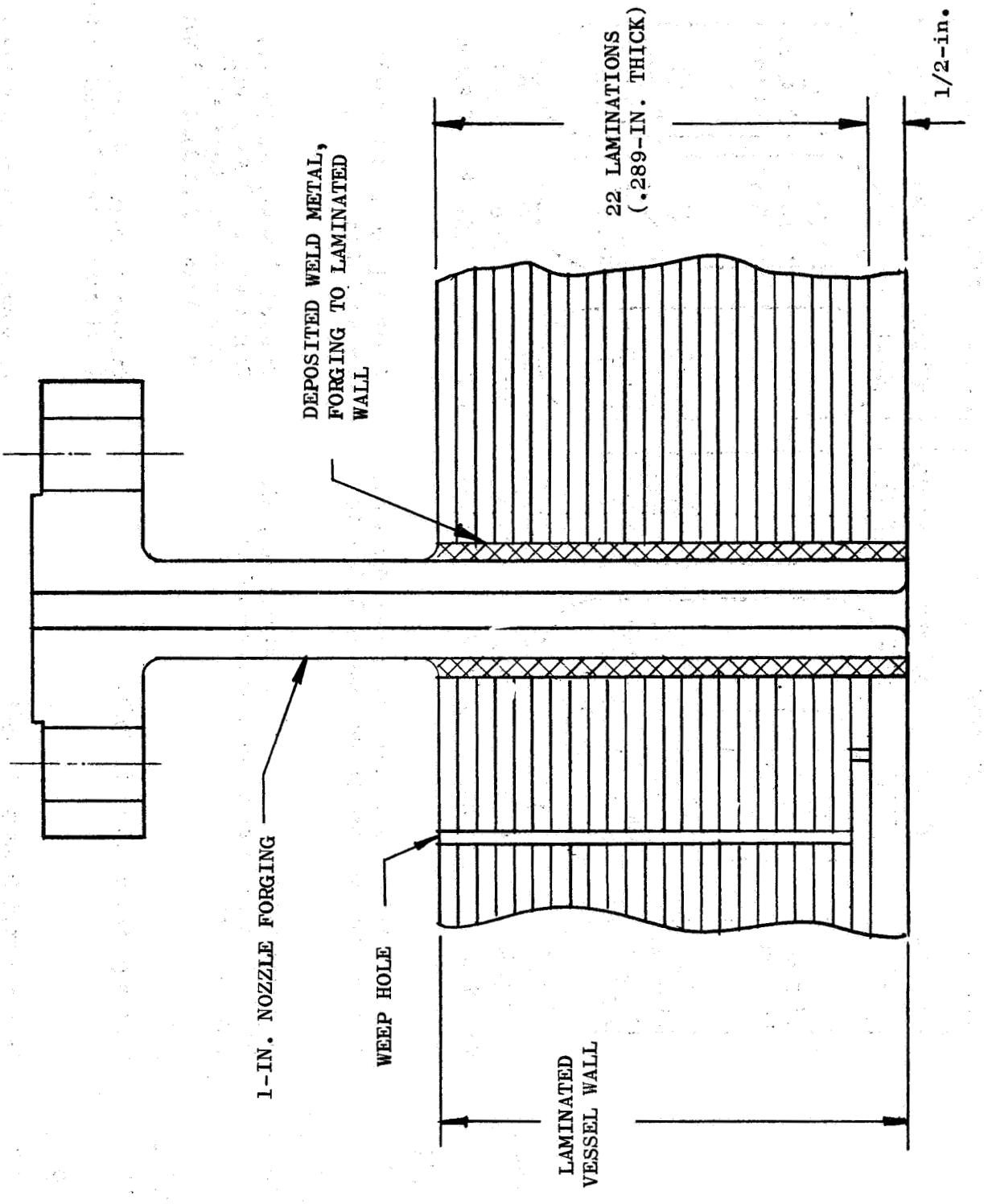

Figure 3

1-in. Nozzle Cross-Section, A.O. Smith 1300 cu. ft. Receiver

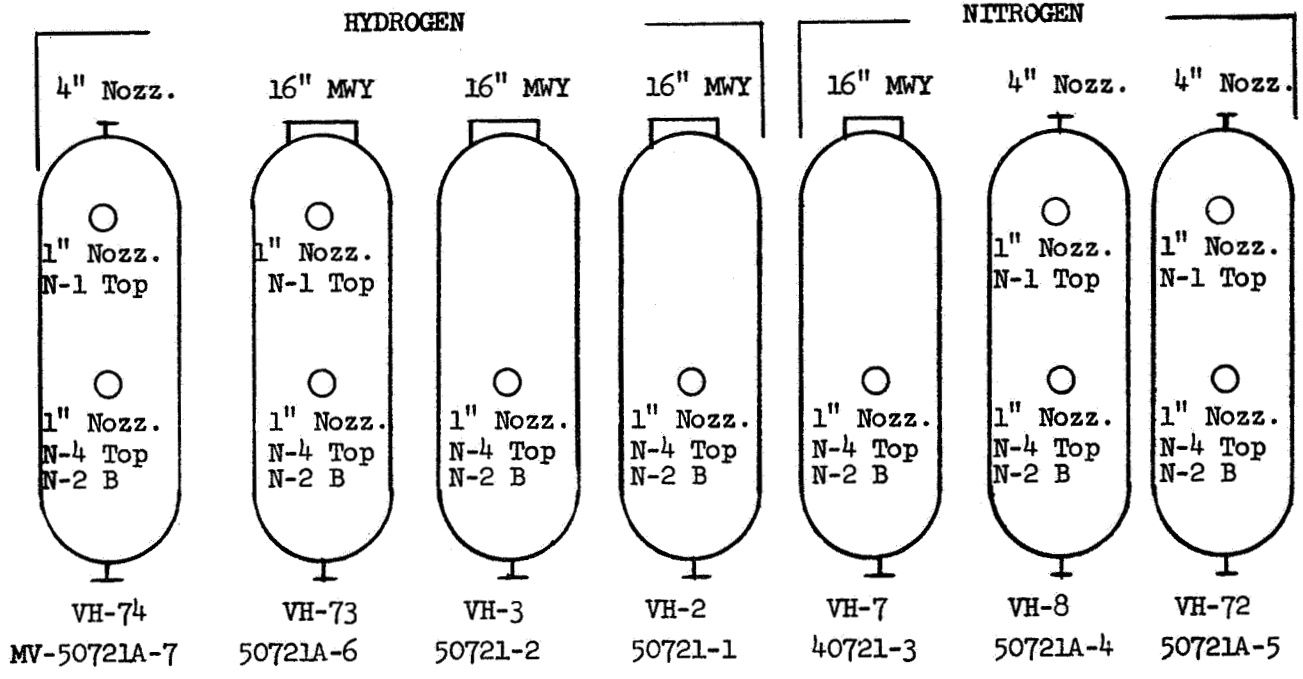

Figure 4
H-8 Test Stand, Vessel Leak History

MV-50721-2

VH-3	Leak reported May 13, 1964. On stream for 9 mo. Failure occurred when pressurized to 4000 psig	Cracked 1" Nozz. N-4 (Top) Replaced Nozz.

MV-50721A-6

VH-73	Leak reported July 28, 1964. On stream July 20, 1964. Failure occurred when pressurized to 4300-4400 psig.	Cracked 1" Nozz. N-2 (Bott.) Deep crack in 8" Nozz. Weld. Replaced Nozz. Repaired 8" Nozz. Weld. Installed 16" MWY.

MV-50721-2

VH-3	Leak reported December 8, 1964.	Cracked 1" Nozz. N-4 Weld. (Replacement Nozz.) Repaired Weld.

MV-50721A-7

VH-74	Leak Reported January 11, 1965.	No manway. Will cut opening in 4" Nozz. head to gain entry and find cause of leak.

SERVICE AND FAILURE HISTORY OF GH_2 STORAGE VESSELS IN TEST AREA H-8

Pressurization History of Vessels*

Month	No. of Times Pressurized	Min/Max Pressure
January 1964	0	0
February 1964	4	1000/3000
March 1964	6	2300/3100
April 1964	10	2300/4200
May 1964	12	1700/4200
June 1964	15	1300/4500
July 1964	16	1600/4500
August 1964	2	800/2900
September 1964	3	1500/2900
October 1964	12	500/4500
December 1964	24	1300/4600

Vessels Placed in Service

Vessel	Date
VH-3, VH-2	September 1963
VH-73, VH-74	July 1964

Vessels Failed

Vessel	Date
VH-3	June 1964 and December 1964
VH-73	July 1964
VH-74	January 1965

* All vessels are the same cycle and pressures from a common manifold in service. Experience with VH-2 in late 1963 could not be established accurately; however, it is believed that only a few cycles at low pressure were involved.

Table 1

C. FAILURE METALLURGICAL INVESTIGATION[1]

1. Nozzle Examination and Removal

A visual examination of the leaking nozzle showed a large radial crack in the nozzle material oriented parallel to the longitudinal axis of the vessel. This crack extended approximately 3-in. up the nozzle bore and broke over the nozzle bore to the vessel inside diameter radius for a distance of approximately 1/3-in. A gap, approximately 0.01-in., was noted between the fractured surfaces. Dye-penetrant inspection showed another crack in the nozzle bore starting approximately 5-1/4-in. This crack was located approximately 130-degrees counter-clockwise from the other crack.

Figure No. 5 is a view of the nozzle showing the open crack. The other crack is located in the bore at the position indicated by the arrow. The contamination visible in the nozzle bore consists of metal chips and cutting fluid which were deposited during removal of the nozzle extension. A 4-1/2-in. inside diameter circular cutter was used to remove a plug containing the nozzle, the entire weld, and a 1/8-in.-thick section through the vessel wall layers. Examination of the plug showed both cracks had progressed to the cut surface. Also, the open crack had closed when removed from the restraint of the vessel wall. The extension of the crack from the bore to the cut surfaces of the vessel laminations is shown on Figures No. 6 and No. 7. Figure No. 6 corresponds to the open crack and Figure No. 7 to the crack restricted to the bore. The actual crack lengths are marked by arrows.

After a preliminary examination, the plug was cut longitudinally into halves, each half containing an entire crack. The open crack shown on Figures No. 5 and No. 6 was submitted by the Test Division to the A. O. Smith Corp. for an independent analysis. The other fracture, the back side of which is shown in Figure No. 7, was retained at Aerojet-General for failure analysis. This portion is presented again in Figures No. 8 and No. 9 to show the extent of cracking; the crack is clearly defined by dye penetrant.

The vessel layers also are shown in Figure No. 9.

2. Examination of the Fractured Surface

The fractured surface was exposed by cutting the sound portion of the nozzle and weld from both ends of the crack and progressively wedging until separation. The open mating surfaces are shown on Figure No. 10; the top and bottom of this figure correspond to those of the nozzle bore. An enlarged view of the fractured surface is shown on Figure No. 11. The saw cut is visible on the left side of the

---

(1) Failure Analysis of GH_2 Pressure Vessel, Aerojet-General Corp. Materials Engineering Report No. FA 65-179, 6 April 1965

Figure 5
View of fractured nozzle from the vessel I.D. The open crack is visible on the lower right. The second crack is located in the bore at the position indicated by the arrow. The contamination in the bore is metal chips from the cutting operation.

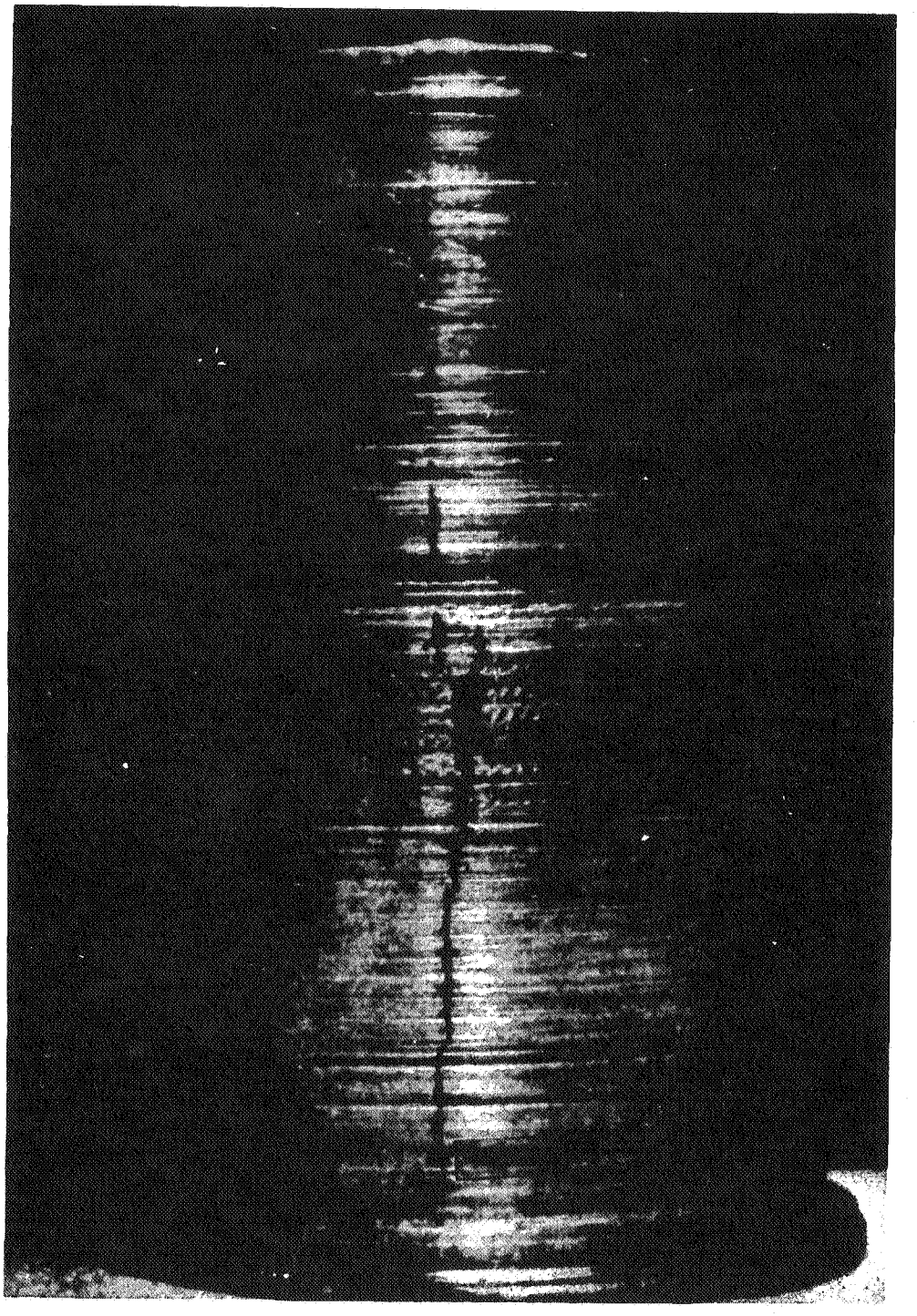

Figure 6
Cut surface of 4¼-in. plug showing extension of the open crack shown in Figure 5. Bottom of the figure corresponds to the vessel I.D. The crack extends between the arrows and is delineated by dry magnetic particle. (Mag: 1.3X)

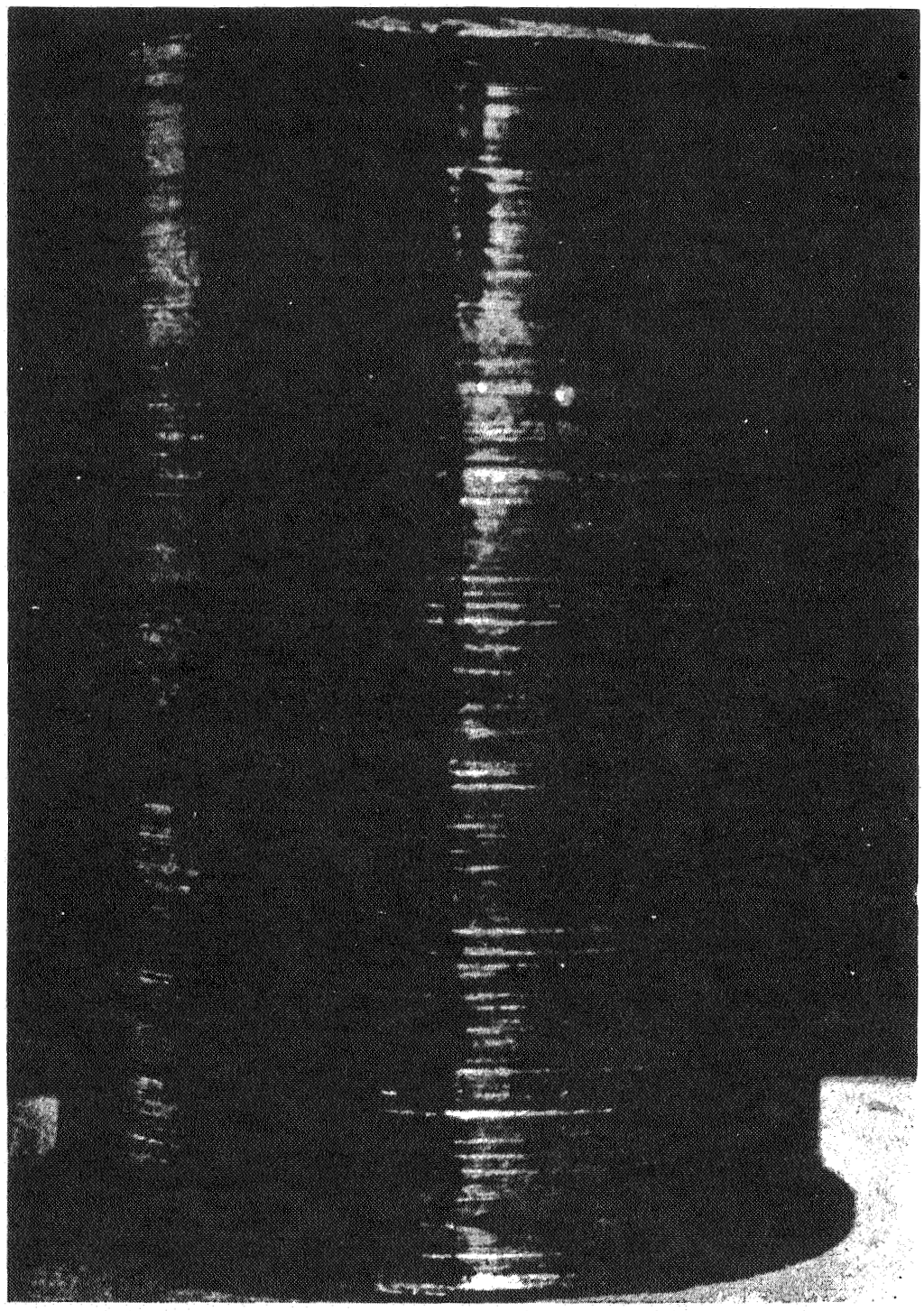

Figure 7
Cut surface of 4¼-in. plug showing the extension of the crack in the nozzle bore. The crack extends between arrows and is delineated by dry magnetic particle. The bottom of the figure corresponds to the vessel I.D. Mag. 1.1X.

Figure 8
Cut Surface of 4-1/4-in. Plug Showing Extension of Crack in the Nozzle Bore (With Dye Penetrant)

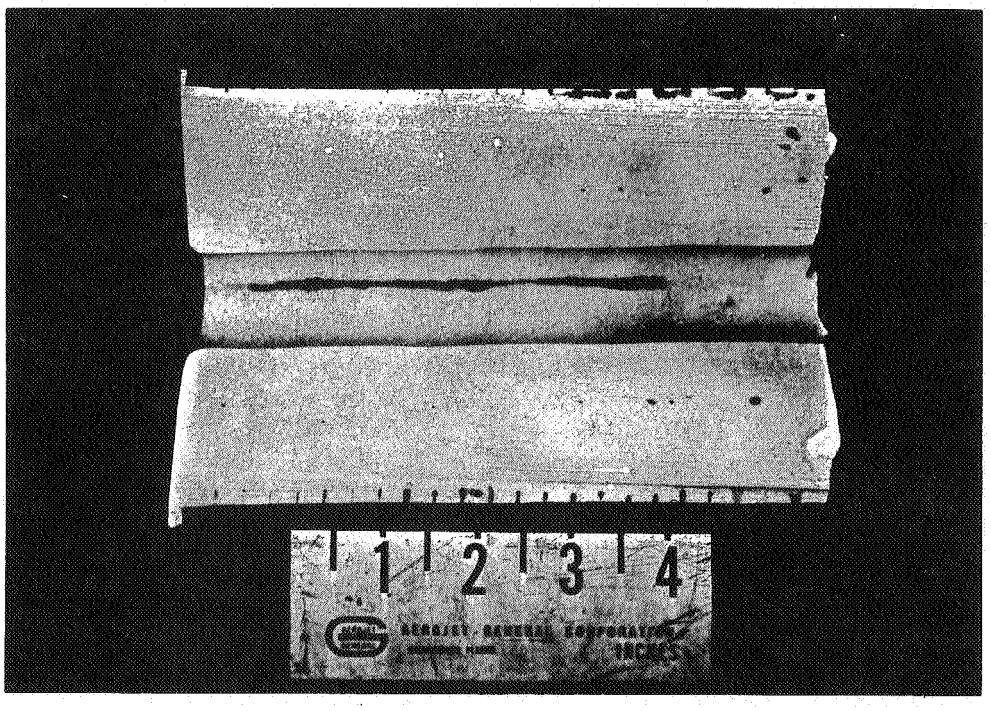

Figure 9
Cross-section showing nozzle bore crack corresponding to the crack shown in Figures 7 and 8. This is also the same crack indicated by the arrow in Figure 5. The left side corresponds to the vessel I.D.

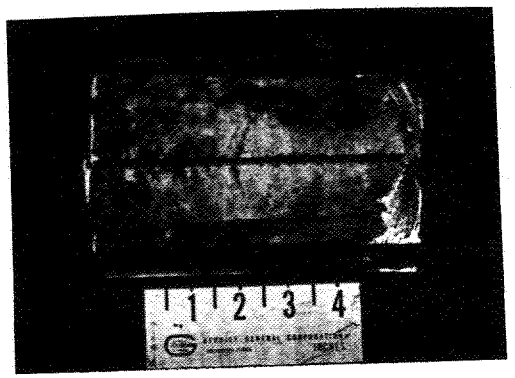

Figure 10

(Left) Mating surfaces of the fracture shown in Figures 7 and 8. The top and bottom of the figure correspond to the nozzle bore.

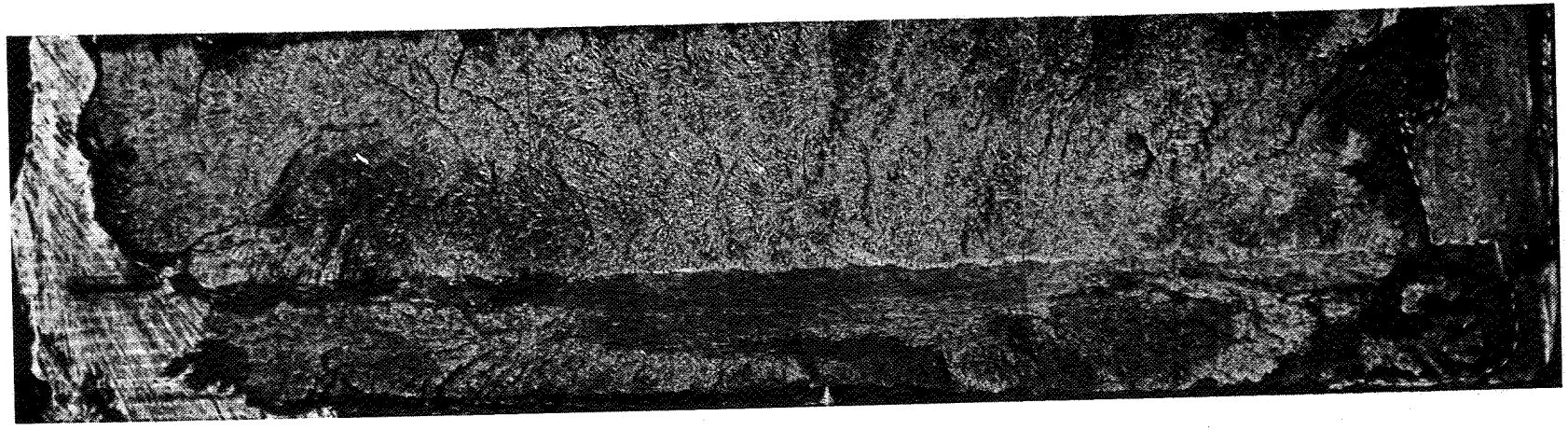

Figure 11

An enlarged view of the fractured surface shown on Figure 10. The saw cut to open the fracture is on the left. The portion fractured to separate the original fracture is outlined in white on the right. The right side is also the vessel I.D. This surface shows staining and oxidation which resulted from atmospheric exposure of the vessel and cutting fluid. The weld nozzle interface is indicated by the arrow at left and extends horizontally across the face. The portion above the arrow is the weld; the portion below, the nozzle. The cross-section at the white arrow is shown in Figure 13. (Mag: 2.5X)

figure as well as on the extreme right. The white outline indicates the area which was fractured in exposing the original fracture. This area also shows staining and oxidization which resulted from atmospheric exposure as well as cutting fluid contamination during the removal operation.

The original fracture surface shows two distinct textures; the flat zone, which extends from the nozzle to weld interface into the central portion of the nozzle material and tapers off at both ends; and the radial zone surrounding the flat zone.

The flat zone, which is a zone of transgranular cleavage also extends partially into the weld zone. This flat zone is visible in the photograph as a light zone in the weld along the weld-nozzle interface.

Examination of the lines in the radial zone indicates that this portion of the fracture radiated catastrophically from all fronts of the cleavage fracture zone. Although the exact origin of the cleavage fracture could not be found, it apparently originated in the central portion of the flat zone, or possibly at the flat zone in the weld. Examination of this area shows no obvious material discontinuities and no evidence characteristic of high temperature hydrogen attack, such as fissuring and fisheyes. It appears that the fracture originated and progressed by cleavage to the extent indicated by the flat portion of the fracture, at which time, this fracture progressed catastrophically from all fronts to the extent indicated by the radial zone. This fracture, on extension to the vessel wall laminations, changes to a ductile mode (see the top of Figure No. 11). The gaps that appear between the laminations are caused by necking of the material at the fracture.

3. Macroexamination and Microexamination

A longitudinal cut was made approximately 1/4-in. behind and parallel to each fractured surface and macroetched. A photograph of this surface is presented as Figure No. 12. The nozzle material is sound and the forging flow lines are evident. Some discontinuities are visible in the weld, but they do not appear excessive for this type of weldment. As shown on Figure No. 12, the nozzle material does not extend completely through the tank; the lower portion of the nozzle is built-up of weld material. The forging flow lines correspond to the longitudinal texturing on the flat fracture surface.

Examination of a longitudinal and transverse section of the fracture surface indicated that the cleavage fracture patch in the nozzle was through a band in the microstructure. A photograph of the transverse mount is shown as Figure No. 13. The left portion of the mount is the weld; the center lighter etching area is the heat-affected zone; and the right portion is the nozzle material. Note the light etching line along the fractured surface on the nozzle. This

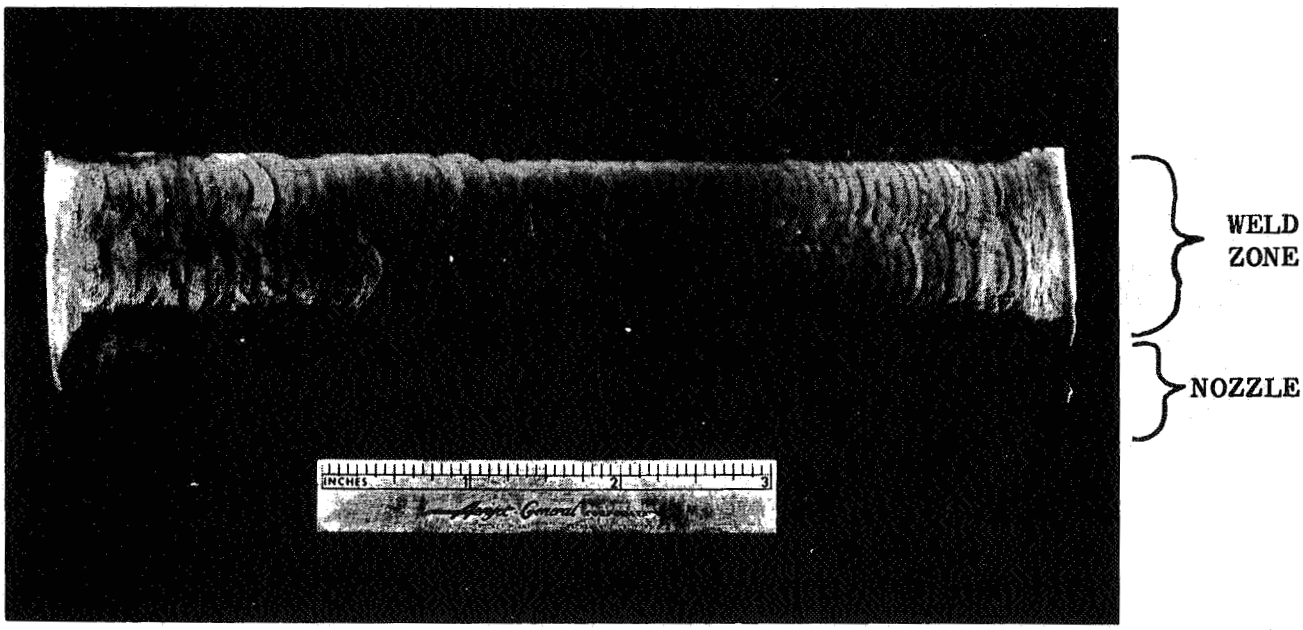

Figure 12

Macroetched cross section of the nozzle and weld.
Left side of figure is vessel I.D.

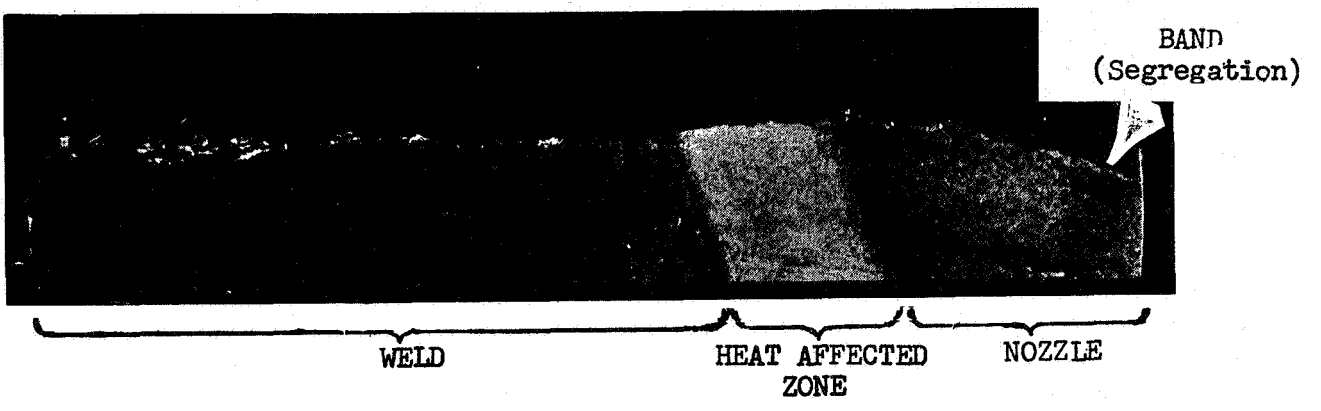

Figure 13

Cross-section of fractures surface showing the flat fracture in the nozzle occurred through a band in the microstructure. This band is visible by the arrow on the right. It extends to the left and meets the fractured surface 1/2-in. left of the arrow and continues along the fractured surface. The light etching center portion is the nozzle HAZ, the left portion is the weld. This cross-section was taken at the white arrow as shown in Figure 11.

Etch: Nital Mag: 6X

line deviates from the fractured surface where the fractured surface changes from flat to radial and is visible in the microstructure by the arrow on the right. A photomicrograph taken of the flat fracture area is shown as Figure No. 14. Note that the microstructure along the fractured surface has a Widmanstatten structure. Further examination shows this structure is common to the cleavage portion of the nozzle fracture. As shown on Figure No. 15, the surface of the radial fracture has a normal distribution of pearlite in a ferrite matrix. A microhardness survey taken along the fracture surface indicated the Widmanstatten structure is somewhat harder than the normal structure. Further microhardness surveys taken on a number of bands confirm this increase in hardness. The chemistry and thermomechanical history of this nozzle indicates that these banded areas are probably high manganese zones carried over from the original ingot manganese segregation. Banding, which is undesirable in a critical location, is not unusual for this type of material because it is a variable quantity as regards magnitude, location, and properties. Figure No. 16 is a photomacrograph of a typical band in the microstructure.

The ASTM E 45 nonmetallic inclusion rating of the 1-in. nozzle is presented below and Figure No. 17 is a representative photograph.

Type A	Type B	Type C	Type D
3T	3T	1T	1T

There are no inclusion specification requirements and the ratings are considered satisfactory. The typical microstructure is shown on Figure No. 18, where the weld microstructure appears sound and normal. As anticipated, no evidence typical of high temperature hydrogen damage, such as microfissuring and decarburization, was noted during the examination.

4. Chemistry

Aerojet-General determined the chemistry of the nozzle and weld material. The results are presented on Table 2 along with the A. O. Smith Corp. 5002 model specification requirement and typical SW 120A composition. The nozzle material conforms to the specification with the exception of the carbon content, which is above the maximum but within the normal allowable check variation. The hydrogen content of both materials is at a low level 0.0001%.

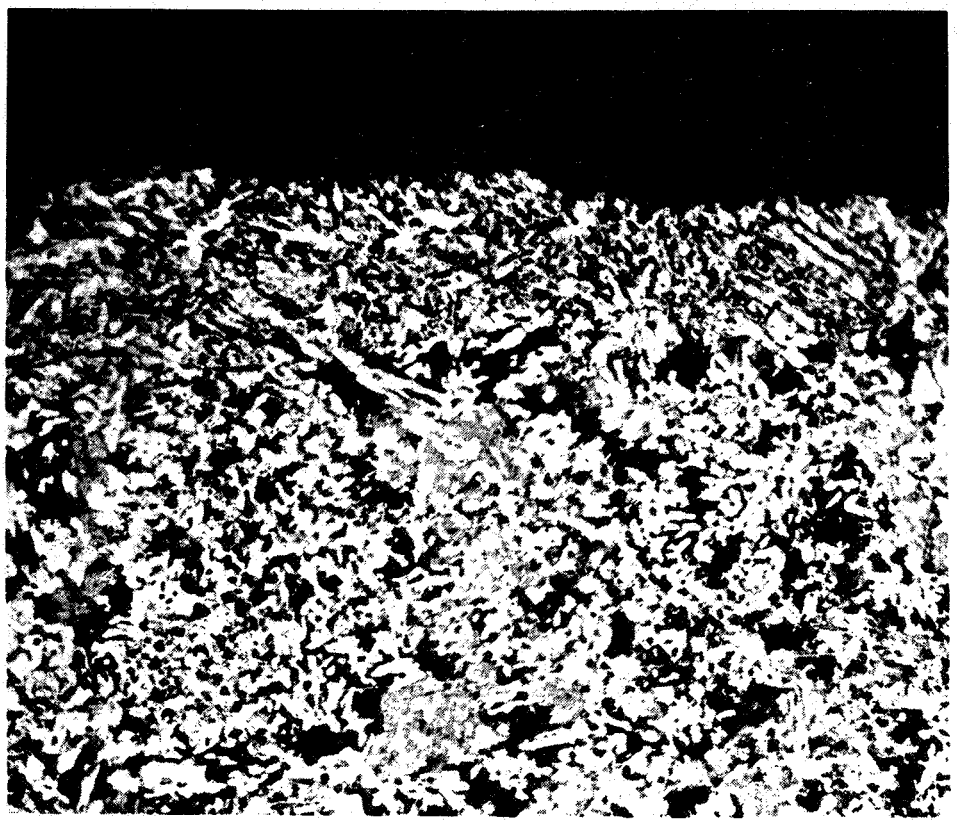

Figure 14

An enlarged view of the fractured surface in the nozzle showing the widmanstatten type of structure. The Knoop hardness in this area was 323. This type of structure was common to the flat fracture in the nozzle.

Etch: Nital Mag: 250X

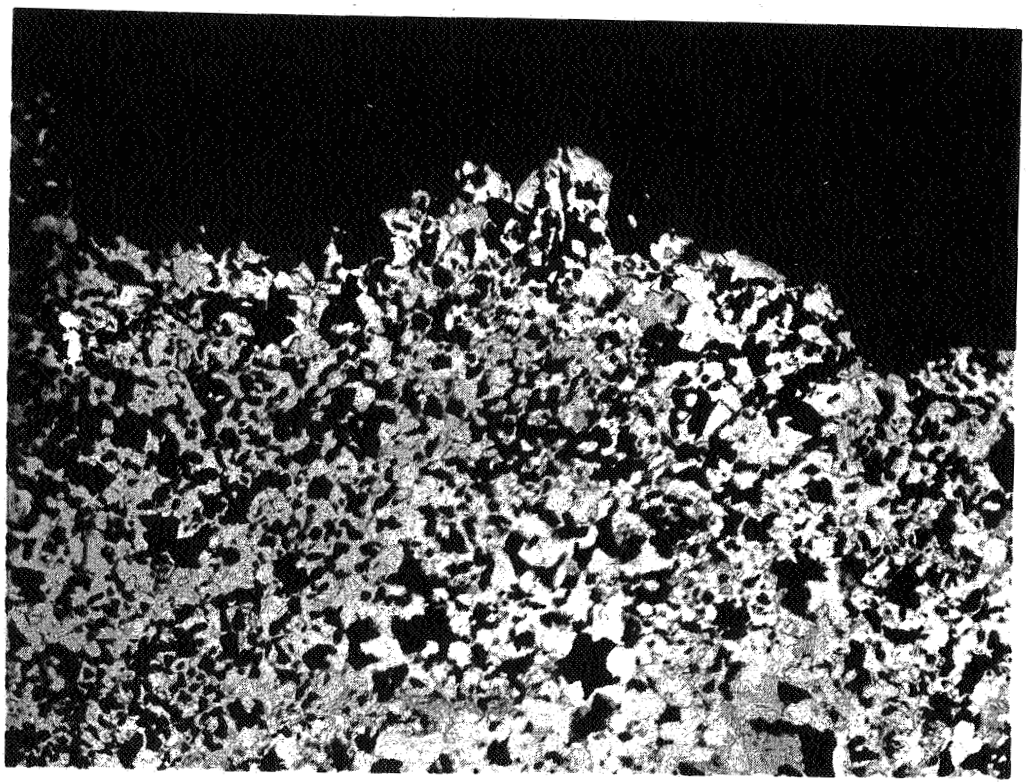

Figure 15: An enlarged view of the fractured surface in the radial fracture zone of the nozzle. The microstructure shows equiaxed pearlite and ferrite. The Knoop hardness in this area was 290. Etch: Nital Mag: 250X

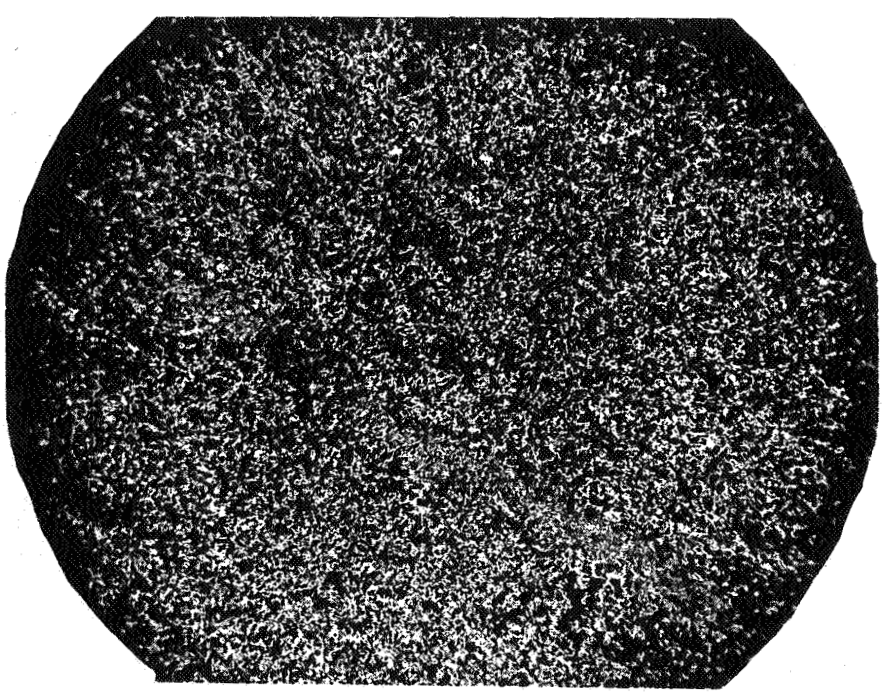

Figure 16: A band in the nozzle microstructure similar to the flat fracture path shown in Figure 14. This band is probably due to manganese segregation. Etch: Nital Mag: 40X

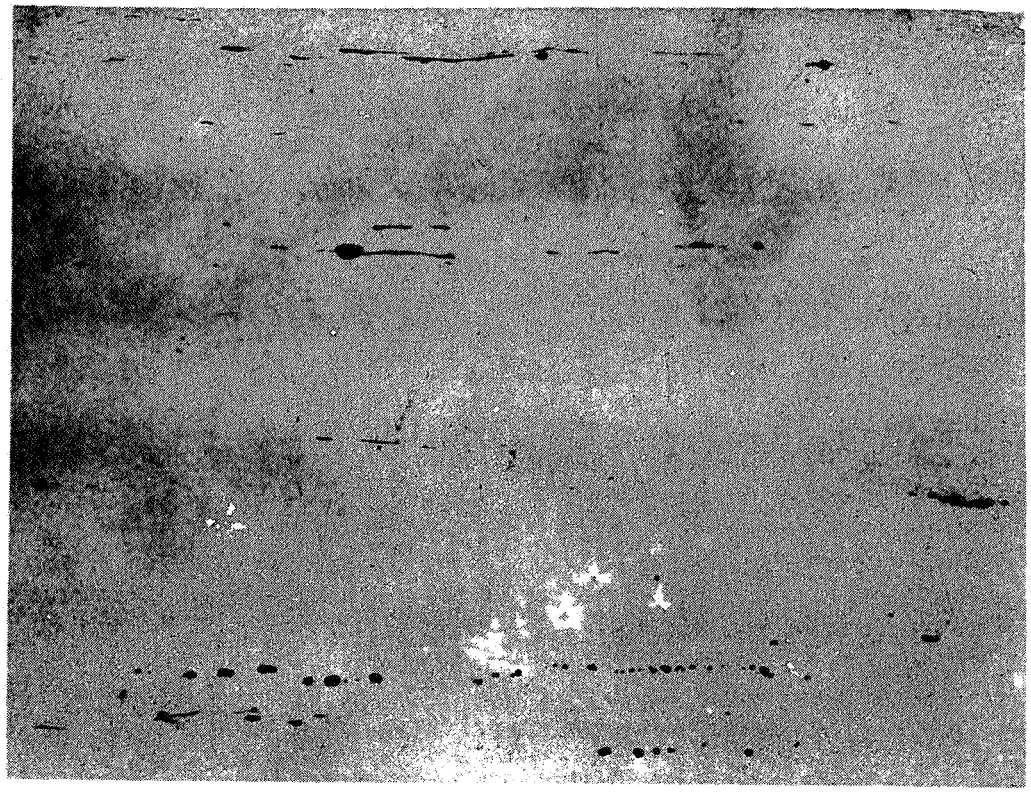

Figure 17: Nonmetallic inclusion content in the nozzle material. It is not excessive for this steel.
Etch: None Mag: 100X

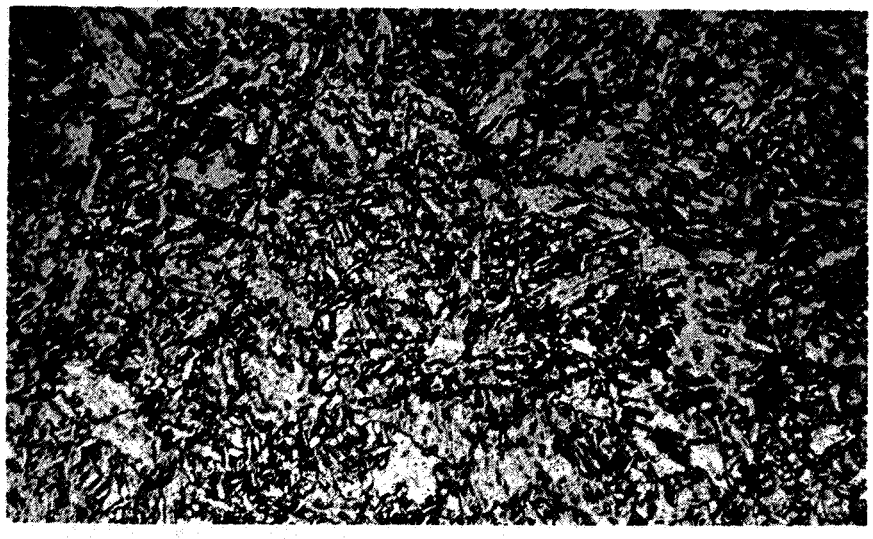

Figure 18: Typical microstructure of the "as-deposited" weld metal.

Table 2

CHEMISTRY OF 1-IN. NOZZLE AND WELD WEIGHT PERCENTAGE

Material	C	S	P	Mn	Si	Cr	Ni	Mo	V	Cu	H_2
1-in. Nozzle AOS 5002 Mod	0.28	0.029	0.007	1.41	0.27	0.04	0.62	-	0.15	0.09	0.0001
Specification Requirement	0.19/ 0.25	0.04 max	0.04 max	1.10/ 1.50	0.020/ 0.35	-	0.40/ 0.70	-	0.13/ 0.18	-	-
Nozzle Weld SW 120A	0.05	0.03	0.004	0.70	0.22	0.03	1.68	0.40	0.20	0.10	0.001
Typical	0.08	0.03 max	0.03 max	0.70	0.34	-	2.00	0.52	0.21	-	-

5. Mechanical Property Tests

Two standard R-4 tensile specimens and a modified R-4 tensile specimen containing a machined V-notch with a K_t of 6.5 were machined from both the nozzle and the weld material. These specimens (gage 7 mm x 1.5 mm diameter) were machined from the nozzle material with tangential orientation. The room temperature tensile test results are presented on Tables 3 and 4. The nozzle material mechanical properties are well above the minimum requirements with excellent ductility indicated. The tangentially-located microtensile specimens were somewhat lower in ductility, which was expected because of the unfavorable forging lines. The increased yield strengths measured on these specimens were partially caused by the increased sensitivity of these smaller specimens to surface cold working during fabrication. The weld material mechanical properties also were good for the limited number of specimens and location.

Four standard V-notched Charpy impact specimens were machined from all-weld material and two were machined from the nozzle. The weld specimens were tested at 75°F, 0°F, -25°F, and -100°F; the nozzle specimens were tested at 75°F and 0°F. The limited results, plotted on Figure No. 19, show that the weld as well as the nozzle has relatively good impact strength at even moderately subzero temperatures. The nozzle material was tested with the impact capacity at 60 ft-lb. Tests at both 75°F and 0°F exceeded this value and additional nozzle material for specimens was not available.

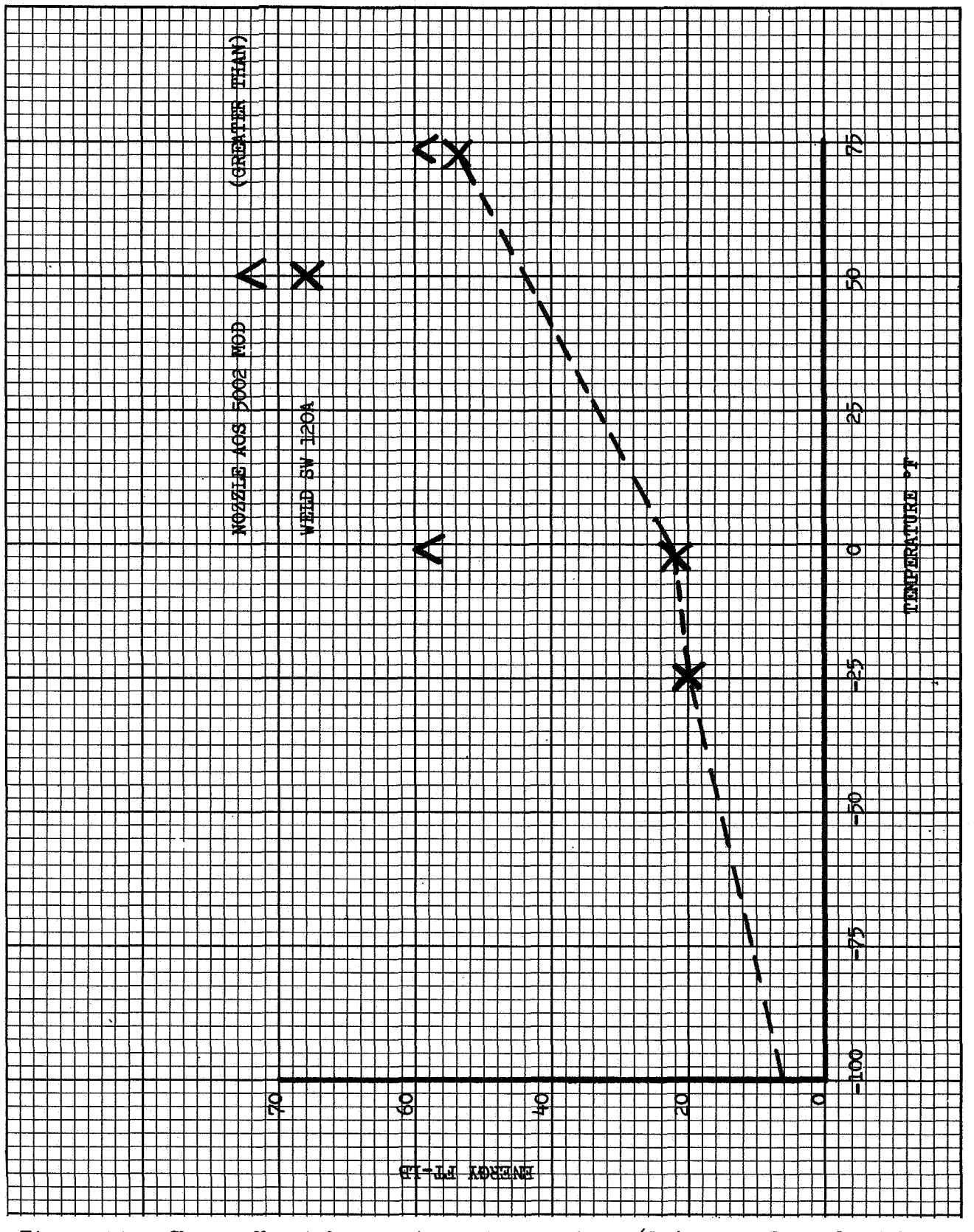

Figure 19: Charpy V-notch Impact vs. Temperature (1-in. nozzle and weld material, VH-74)

Table 3

TENSILE PROPERTIES OF ONE-INCH NOZZLE AND WELD*

Material	Specimen Orientation	UTS ksi	0.2% U.S. ksi	Elongation %	RA	Hardness
1-in. Nozzle	Longitudinal	109	66	26	65	R_A 60.5
AOS 5002 Mod	Longitudinal	106	65	28	65	R_A 59.5
1-in. Nozzle	Tangential	105	74	19	48	--
AOS 5002 Mod	Tangential	103	74	20	51	--
Specification Requirement	--	80 min	51 min	18 min	35 min	
SW 120A 1-in. Nozzle Weld	--	112	102	20	64	R_A 61.5
	--	114	101	16	62	R_A 64.0

* One-inch nozzle tangential specimens were microtensile (gage 7 mm x 1.5 mm dia.). All others were standard R-4.

Table 4

NOTCHED TENSILE STRENGTH OF ONE-INCH NOZZLE AND WELD

Material	Specimen Orientation	NTS ksi	K_T (Petersons)	NTS/UTS Ave.
1-in. Nozzle	Longitudinal	141	6.5	1.3
Weld	Longitudinal	170	6.5	1.5

6. Discussion of Test Results

The test results indicate that both the nozzle and weld have satisfactory chemical and mechanical properties in accordance with the specification requirements. Limited impact test results show that low temperature brittleness should not be a problem down to -25°F and probably to even lower temperatures. The chemical segregation (banding) noted in the nozzle material appears heavy, but is not unexpected in this material with 1.10% to 1.50% manganese content because manganese has a tendency to segregate in the original ingot cooling. These high manganese areas are difficult to eliminate because manganese tends to form a substitutional solid solution in austenite and has a slow

diffusion rate; therefore, the segregate can be carried to the finished product. These high manganese areas appear to have resulted in a Widmanstatten transformation structure when cooled from the normalizing temperatures. The microstructure appears to be partially bainitic, and combined with the strengthening effect of the manganese, can result in the increased hardness measured in these areas.

Examination of the fracture indicates that cracking originated and progressed by transgranular cleavage either from the interior of the nozzle or possibly from the cleavage portion of the weld until it reached a critical size. The fracture then radiated catastrophically from all fronts of the existing crack. It also was noted that the cleavage fracture path was directly through a band in the nozzle microstructure. This banded area was somewhat harder than the surrounding matrix. A review of the vessel history shows that the vessel passed a 7500 psi hydrostatic proof test and performed satisfactorily for five months prior to failure. The failure occurred on 11 January 1965 while sustaining 4600 psi of hydrogen gas. The failure occurred at an ambient temperature of 51°F. The last activity concerning this tank was 72 hours before the failure when the gas filling operation was completed.

The vessel history and failure investigation indicate the vessel failed because of a delayed failure mechanism that resulted in the initiation and propagation of a cleavage fracture. The possible metallurgical mechanisms which may be considered are: stress corrosion cracking, high or low cycle fatigue, low temperature embrittlement, and hydrogen embrittlement by high pressure hydrogen gas.

a. Stress Corrosion

Stress corrosion appears unlikely in this failure because the fracture appears to have originated from the interior of the material, progressed by cleavage, and there is no evidence of corrosion on the inside surfaces of the tank. Stress corrosion of these materials is associated with surface chemical reactions and primarily results in a transgranular fracture.

b. Fatigue

Classical fatigue failure, that is failure occurring after a large number of load cycles (10,000 or more), can be discounted because an insufficient number of load cycles occurred and no fatigue striations were found on the fractured surface by macrographic and fractographic examination. However, the possibility of low cycle fatigue was considered because the cyclic nature of operation apparently influenced the initiation and propogation of the failure and there is greater susceptibility to this mode of failure in zones of higher strength banding. Low cycle fatigue is similar to static failure and is a process of course "slip" occurring at high stress levels at stress risers in an area of high stress. Only the hydrogen vessels have suffered failures and at various cyclic histories. Three identical nitrogen

receivers that were fabricated in the same lot as the hydrogen units were subjected to greater average pressure (and stress) as well as a larger number of cycles without failure. In addition, the A. O. Smith Corp. reported that scores of receivers with identical or similar nozzle designs, loaded to equal or higher stresses in a wide variety of applications have been in service for years without a comparable failure. This evidence indicates that low cycle fatigue alone is inadequate to explain the failures nor can low cycle fatigue be completely eliminated. It is conceivable that the random accumulation of fabrication and material differences could have combined in a manner which could cause the statistical disparity between the hydrogen experience and that with all the other gases.

c. Low Temperature Embrittlement

Low temperature embrittlement also appears unlikely based upon the results of the temperature fluctuations measured on the vessels during operation.

Temperatures have been measured at two locations. In one of these a single thermocouple is inserted into a receiver shell "weep hole" which is located three feet from the 2-in. nozzle, to the depth of the outer surface of the second layer, or to a point approximately 0.8-in. from the inner surface of the vessel. The temperature changes noted at this location for 48 hours of normal operation varied in a lagging cycle with the ambient temperature (30°F change) with significantly less spread (less than 10°F).

The second location for temperature measurement is a four-thermocouple installation in the copper ring gasket between one receiver discharge nozzle and an 8-in. shut-off valve. Two thermocouples are flush with the inner diameter of the ring; two project into the gas flow stream at the nozzle inner diameter. In flow test No. 6.0-05-EHM-007, which was performed on 9 December 1965, the gaseous hydrogen flow rate per receiver varied from 30 lb/sec to 8 lb/sec over a 20 sec period and was accompanied by a pressure reduction from 3000 psi to 2000 psi. During this test, the average temperature reduction of the two projecting thermocouples was 20°F (from the pre-test temperature of 45°F) and for the two flush thermocouples, it was only 2°F.

Although these data do now show the precise temperature fluctuations at the inlet to the 1-in. nozzle, they do indicate that the expansion-induced temperature changes in the nozzle material are probably not severe enough to cause embrittlement. This is reinforced by the fact that there were no vent cycles through the 1-in. nozzles.

A review of the test results shows a ductile-to-brittle transition temperature of well below 0°F for both materials. The lowest ambient temperature recorded during the three days prior to failure was 40°F. The temperature at the time of vessel failure was approximately

50°F, with the latest tank activity (gas filling) occurring 72 hours before the failure.

d. Hydrogen Embrittlement by High-Pressure Hydrogen Gas

The effect of hydrogen upon the properties of steels is a recognized phenomenon and can be classified into two general categories; hydrogen attack and hydrogen embrittlement.

Hydrogen attack is caused by chemical reaction between the hydrogen and the carbon in steels and results in permanent degradation of properties. This type of attack generally occurs at temperatures above 425°F and damage can be readily detected by examining the steel. No evidence of this type of damage was detected on the nozzle or weld material.

Hydrogen embrittlement effect is caused by the presence of hydrogen in the steel. If undamaged during the presence of hydrogen, the steel can recover from this effect when the hydrogen is removed. This effusion of hydrogen occurs rapidly upon the removal of the hydrogen source even at room temperature, unless this process is hindered by low temperatures or an application of a low permeability coating, or plating. Testing of this material subsequent to the effusion of hydrogen, such as is the case in testing these tank materials, will not disclose the temporary embrittling effect suffered by the material. In a discussion of the mechanisms and factors affecting hydrogen embrittlement, D. P. Smith[2] states that the strength level of the steel is the most important factor affecting the occurrence of hydrogen embrittlement. Both the minimum stress required to produce a crack and the minimum incubation time required to initiate the crack are decreased as the strength of the steel increases. This dependency upon the strength level also is reported to be independent of microstructure and chemistry. These characteristics were developed primarily from electrolytically-charged specimens but they should be independent of the hydrogen source except for the wide differences that may exist in driving force and time constants between cathodic and high pressure conditions (above 3500 psi in the context of this report).

The delayed catastrophic failure of steels by hydrogen embrittlement occurs when a critical combination of stress, hydrogen concentration, and time is exceeded.

Only limited information was found regarding the effect of high pressure hydrogen gas upon low alloy steels and these were not concerned with the pressures at 5000 psi. However, available information[3] indicates that high pressure molecular hydrogen gas as low as

(2) Smith, D. P., Hydrogen in Metals, University of Chicago Press, Chicago, Ill., 1948

(3) Smialowski, M., Hydrogen in Steel, Addison-Wesley Publishing Co., Reading, Mass., 1962

2250 psi can affect the measured ductility of normalized 0.22% carbon steel. Additional research by H. C. Van Ness[4] and others[5] have shown that C1025 at 65 ksi tensile strength has up to a 25% loss in notched tensile strength when tested under 10,000 psi hydrogen gas pressure. As stated previously, this type of testing is very limited, but it does show that pressures as low as 2750 psi hydrogen gas is sufficient to produce a measurable change in the ductility of materials of the type used in the vessels at even lower strength levels than the 1-in. nozzle or the associated weld. This effect, in the absence of high stress levels, probably does not affect the performance of lower strength alloy steels of the type used in the vessel construction. However, in the 1-in. nozzle area, it appears that the critical stress level to produce catastrophic failure was supplied by the unrelieved welding stresses combined with the additive effect of the operational stresses. This is supported by the observed gap between the fractured surface of the nozzle crack which closed when removed from the restraint of the vessel walls. Possible evidence of hydrogen embrittlement is provided by the fracture path in the nozzle. This fracture path occurred in a high alloy band which, because of its increased hardness, is more susceptible to this type of embrittling phenomenon.

The banding of the nozzle material is not considered significant. The critical condition of the 1-in. nozzle and weld area is caused by the high level of residual stress and would provide a marginal condition even for unbanded materials. The high level of residual stress in this area will have to be eliminated or reduced as much as practical to lessen the possibility of repeated failures.

D. STRESS INVESTIGATION

As a result of the cracking problem associated with the gaseous hydrogen receiver tanks, a structural analysis was made of the stress distribution that can be expected to exist in the vicinity of the 1-in. nozzle. Two major types of stress were analyzed; the residual stress resulting from fabrication and the applied stress resulting from the application of internal pressure. The residual stresses in the tank can be separated into two categories; the stresses resulting from the laminated construction of the basic cylindrical shell and the stresses resulting from the welding in place of the 1-in. nozzle.

---

(4) Van Ness, H. C., and Dodge, B. F., "Effects at High Pressures on the Mechanical Properties of Metals." Chem. Engr. Progress, V. 51, n. 6, pp. 266-271, June 1955.

(5) Perlmutter, D. D., and Dodge, B. F., "Effects of Hydrogen on Properties of Metals," Ind. and Engr. Chem., V. 48, n. 5, pp. 885-893, May 1956

1. Residual Stresses

a. Residual Stresses Resulting from Laminated Construction

Discussion with the manufacturer indicated the following general fabrication technique. The 1/2-in. inner layer is welded into a cylindrical shell, and the additional layers, 0.289-in. thick, are then applied with considerable pre-tensions in them. The pre-tension value might be as high as 10,000 psi. Because of the apparent lack of precise control in the pre-tensioning process, it is assumed that the pre-tension during fabrication can vary between zero and 10,000 psi at any particular location. As a limiting condition, the residual stress distribution has been computed for an assumed 10,000-psi pre-tension in each sheet as it is applied.

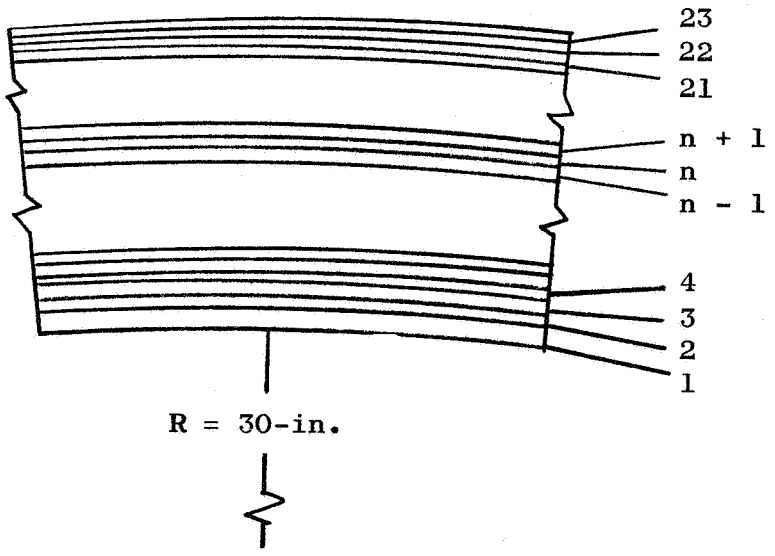

Consider the residual stress induced by the application of the n^{th} layer:

$$\sigma P.C. \quad \frac{t_n}{t_1 + t_2 \ldots t_n - 1} \quad x \ \sigma P.T.$$

Where

$\sigma P.C.$ = the increment of pre-compression applied to all existing layers because of the application of the n^{th} layer.

t = thickness of appropriate layers as designed by subscripts.

$\sigma P_o T_o$ = the pre-tension in the $n^{\underline{th}}$ layer as it is applied.

To obtain the total pre-stress in any layer n after all wraps have been applied, the following expression can be written:

$$\sigma P.S. = \sigma P_o T_o - \sum_{m=n+1}^{m=23} \sigma P.C.$$

The above expression has been evaluated for all layers and a plot of the final pre-stress as a function of radial locations is shown on Figure No. 20. From this plot, it is seen that the pre-compression reaches a maximum of approximately 27,000 psi at the inner surface of the shell.

b. Residual Stresses Resulting from Welding

The design of the nozzle weld is such that any shrinkage of the weld metal from its "as-deposited" condition will generate residual stresses. To evaluate the possible magnitude of these stresses, the temperature distribution indicated below was assumed to be applicable for the "as-deposited" weld metal. The stresses caused by this temperature distribution cooling to ambient were then computed by means of a digital computer program designed for evaluating thermal stresses in solid rocket nozzle inserts.

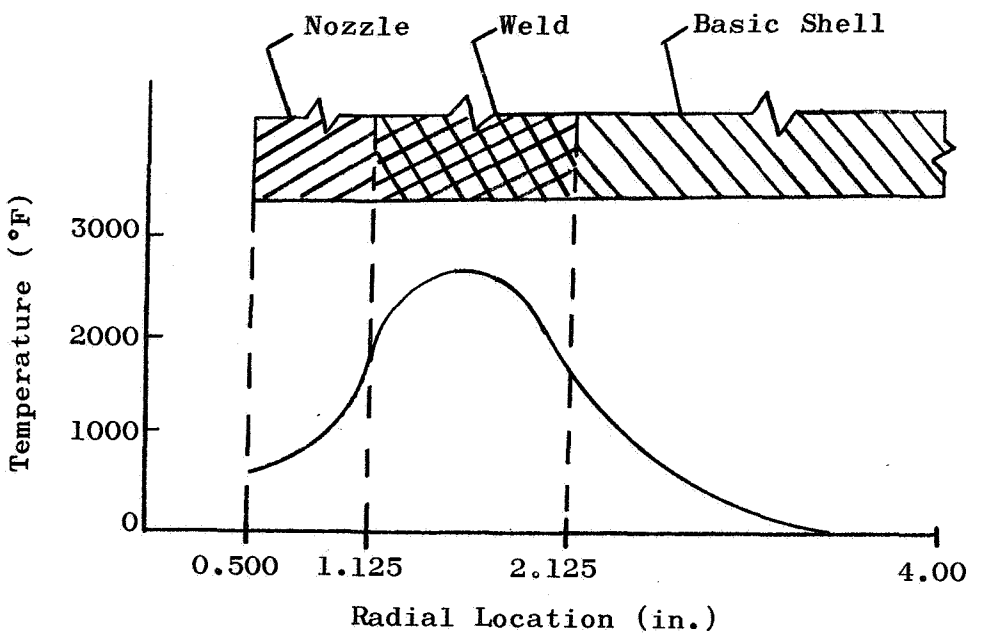

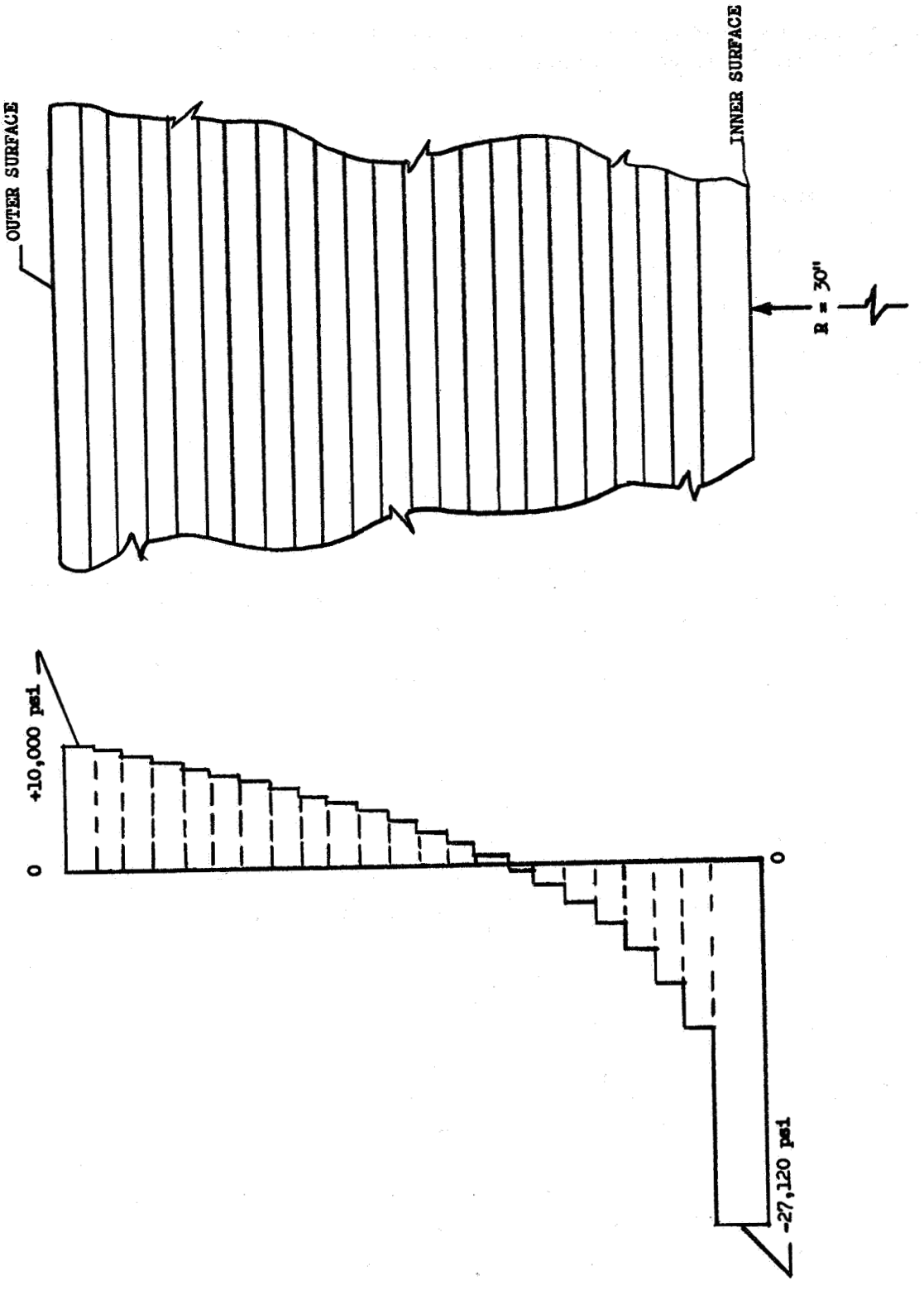

Figure 20: Hoop Stress Distribution Attributable to Pre-load Operation in Manufacture

The effective modulus of elasticity used in the thermal stress calculation was the secant modulus based upon the "ΔT" strain at the point under consideration. A plot of this modulus as a function of temperature is indicated below:

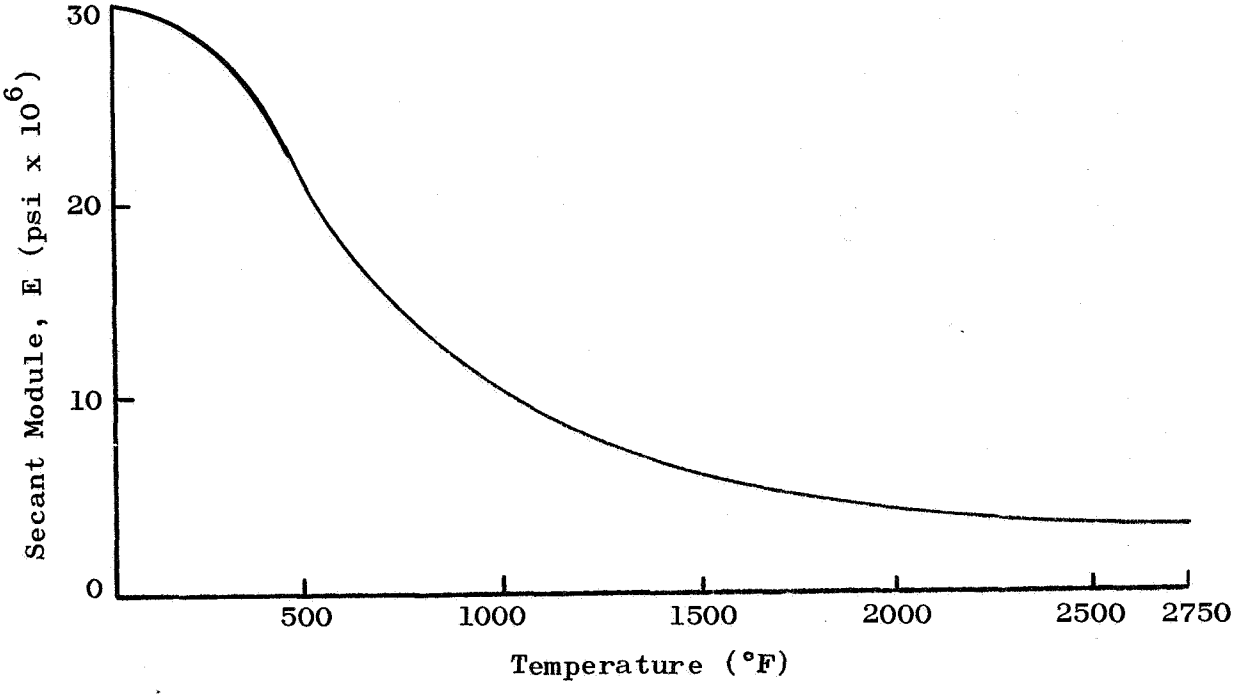

To account for the difference in radial restraint that will exist through the weld, both plane stress and plane strain solutions were made. The plane stress solution is considered applicable to the outer weld layers while the plane strain solution is applicable to the interior layers. Results of these solutions are shown on Figure No. 21. In both solutions, it is seen that the maximum residual stresses are well above the elastic limit of the material with the plane strain solution producing a condition of triaxial tension having all three components of normal stress above the yield strength of the material.

2. Applied Stresses

The applied stress distribution around the nozzle is directly dependent upon the basic stress distribution in the cylindrical shell. This shell stress, in turn, depends upon the fit and pre-stress of the various layers. Because the exact fabrication procedure is unknown, a check was made for two different assumed conditions.

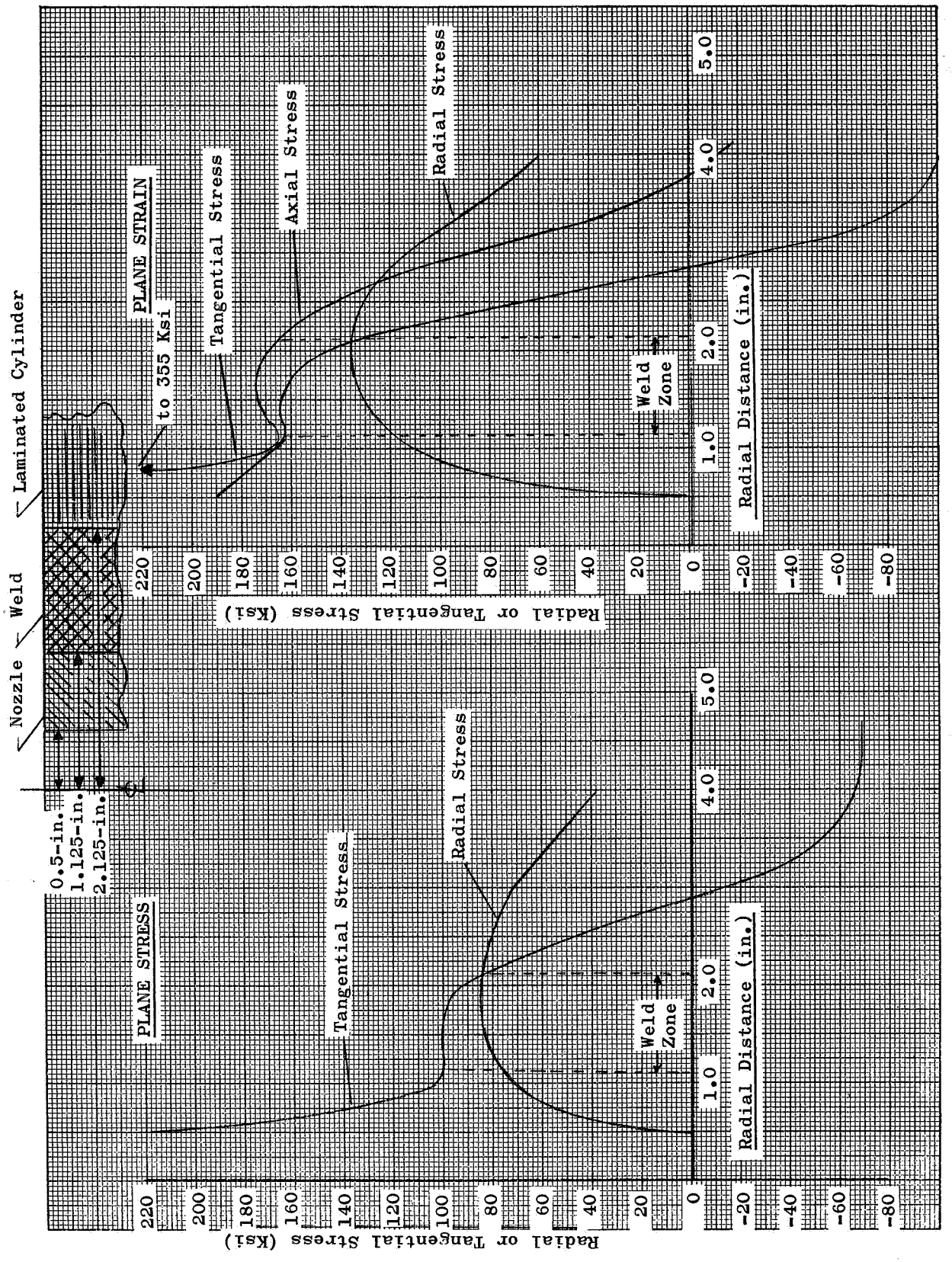

Figure 21: Stress Distribution Radially-Outward from Nozzle Centerline

a. The first condition is with all layers in contact but no pre-stress in any layer. This condition results in the same stress distribution as that for a homogeneous cylinder and can be defined as follows:

$$\sigma_{\Theta} = p \frac{a^2 (b^2 + r^2)}{r^2 (b^2 - a^2)}$$

where:

σ_{Θ} = tangential stress

p = internal pressure

a = inside radius

b = outside radius

r = radius of point in question

b. The second condition is with all layers in contact with 10,000 psi tensile stress applied to each layer during fabrication. This condition results in the same stress distribution as indicated for the first condition being superimposed upon the residual stress distribution shown on Figure No. 20.

Plots of the tangential stress distribution in the basic cylinder for each of the above conditions are shown on Figure No. 21. In the vicinity of the 1-in. nozzle, the stress distribution in the basic cylinder will be modified by the presence of the hole. For a 2:1 biaxial stress field, such as exists in cylindrical pressure vessels, the tangential stress at the edge of the hole is increased over the nominal stress by a factor of 2-1/2. This would result in the stress distribution shown on Figure No. 22 being multiplied by 2-1/2 to obtain the maximum values at the inside edge of the nozzle opening.

3. Discussion of Results

During operation, the total stress field in the vicinity of the 1-in. nozzle normally would be the combination of the residual and applied stresses. However, one or both of these stresses will be above the yield strength of the material depending upon the fabrication procedure. Where the opportunity exists for plastic flow to take place, such as at the inside edge of the nozzle opening, the maximum stress is expected to be very close to the yield strength of the nozzle material (approximately 70,000 psi). However, the strain would be increased from the elastic equivalent of 70,000 psi stress. Based upon an approximate conversion from stress to strain, the maximum residual strain caused by welding would be 0.61% at the inside edge of the nozzle opening. Depending upon the amount of pre-stress in the basic tank construction,

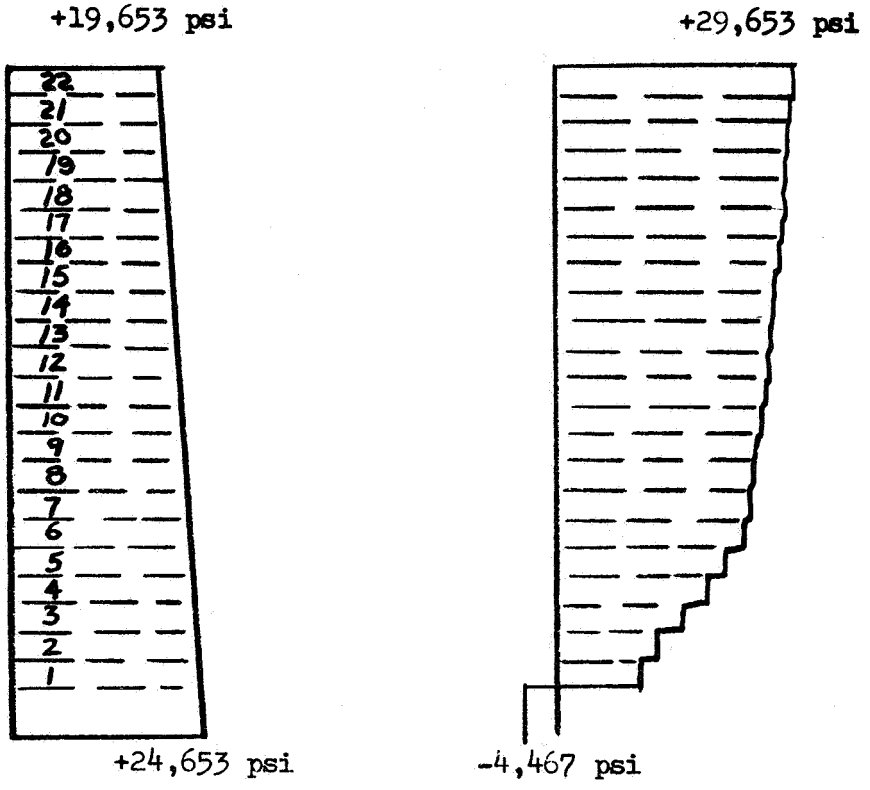

Figure 22: Hoop Stress Distribution Through Thickness of Cylinder

the maximum applied strain at this point would be between -0.9% and +0.78%. Considering the worst possibility, the maximum tangential strain at the edge of the nozzle opening would be 1.39%, with 0.78% of this being of a cyclic nature. Normally, this condition, while undesirable, is apparently not too serious for a material having approximately a 25% elongation.

For the interior of the nozzle weld, the situation is somewhat different. Because of the triaxial stress field, plastic flow of the material will be prevented and stresses well above the yield point of the material can exist. This condition, while not necessarily detrimental in itself, is highly conducive to the propagation of flaws or cracks. It is used in test specimens for crack-propagation studies.

In summary, the analysis of the 1-in. nozzle area indicated the following:

a. Residual stresses in the central portion of nozzle weld cause a state of triaxial tension with all components of principal stress above the yield strength of the material.

b. Residual stresses at the inside edge of the nozzle opening will be at the tensile yield strength of the material and the material will be strained approximately 0.60%.

c. Applied stresses at the inside edge of the nozzle caused by pressure can vary from slight compression to an intermediate tension stress, depending upon the efficiency and consistency of fabrication.

IV. CONCLUSIONS

A. No conclusive single cause of failure was ascertained for the failure of the A. O. Smith vessels. The following are the results from the combined metallurgical investigation, stress analysis, and literature search.

1. Metallurgical examination revealed a transgranular cleavage at the origin of the nozzle failure and located along the nozzle-weld interface. The cleavage progressed into the nozzle material along a segregation band.

2. Triaxial stresses, which result from the geometry and the manner of fabrication, were calculated. The possible stresses were found to be well above the yield point within the weld.

3. A survey of the literature shows that materials of construction commonly used in the fabrication of high-pressure gas receivers can be subject to adverse changes in strength properties upon exposure to high-pressure hydrogen gas. This effect appears to be related to gas pressure, time of exposure, stress level, as well as the

basic condition and properties of the material. Hydrogen effect (embrittlement) is aggravated in areas of residual welding stress and at high operating stress levels, as well as by surface stress risers (i.e., micro-cracks, notches, or other discontinuities). This effect becomes larger as the yield strength of the material increases. A threshold of either pressure or time for increments of strength degradation of a material by hydrogen cannot be properly defined with the available data. These conditions, coupled with the successful use of vessels of the same design with nitrogen, indicate that hydrogen embrittlement is a highly probable cause of failure.

4. The concept of failure as the result of low cycle fatigue also is supported by the location of the failure origin as well as the attendant high triaxial stresses at that location. This high stress could differ from vessel to vessel, but such differences should not be significant with the standard fabrication techniques used.

B. The failures of the high-pressure storage vessels reported herein reveal areas of concern that require the attention of both potential suppliers and users of such vessels. It is possible that the structural design is inadequately controlled by the existing applicable codes. Fabrication as well as inspection must be more clearly defined and implemented to enable the production of a quality end product. Also, the quantitative effects of the atmospheres to be contained upon the properties of the materials of construction must be determined.

V. RECOMMENDATIONS

The following recommendations deal with high-pressure gas receivers and with the adverse effect of embrittlement of metals by gaseous hydrogen in the basic areas of facilities storage. Related, but more sophisticated areas of association between hydrogen gas and alloy steels (i.e., those in rotating machinery and compressors) are beyond the scope of this report.

A. GENERAL PROBLEM AREAS REQUIRING FURTHER ACTION

1. The determination of the hydrogen relationship to existing materials and installations.

2. The determination of corrective modifications and the need for periodic inspections to ensure safe operation of existing installations.

3. The conduct of government-supported research or an investigative program to establish adequate parametric information to guide future designs.

4. The incorporation of the essential elements of the new information into the applicable pressure vessel, piping, and welding codes in the form of appropriate limitations as well as the strengthening

of these codes in the known areas of deficiency involving residual stresses.

B. SPECIFIC CORRECTIVE ACTIONS

Specific recommendations which expand upon the above first two general areas are:

1. Perform an immediate and simplified investigation to determine the conditions under which high pressure gaseous hydrogen will embrittle selected alloys and austenitic stainless steel at ambient temperature. Utilize notched test specimens of both welded and basic materials tensile loaded in special equipment permitting simultaneous application of pressure conditions and test load. The following priority test materials are proposed:

ASTM - A - 302	U.S. Steel T-1
ASTM - A - 212	ASTM - A - 106, Gr B
A.O. Smith 1146A	AISI 304L

2. Incorporate access man-ways in all hydrogen gas receivers utilized at pressures above 3600 psi; establish a six-month depressurization and internal inspection cycle for each of these units on a government-industry coordinated plan basis. Continue this inspection cycle based upon the future evaluation of inspection results and the metallurgical investigation of the materials listed above.

3. Review the ASME Unfired Pressure Vessel Code in a joint Industry/Government Committee action to:

a. Increase the analytical requirements of Section VIII (perhaps to that of Section III) to avoid designs producing localized, high residual stresses.

b. Vessel designs utilizing multi-layer construction are encouraged to avoid the installation of accessory nozzles or other openings in the laminated wall. The preferential location is the forged head area. Dip-tubes could be used, if required, for low-point drains, thereby permitting the drain nozzle to be located in the solid head.

c. Require designer/fabricator to demonstrate material-to-gas (or liquid) compatibility in all cases.

4. Recommendation for specific corrective action for the individual multilayer receivers that have failed, particularly the vessel VH-74, have been separately processed. Briefly, these corrective action recommendations have pertained to the elimination or correction to the critical 1-in. nozzle area and, with the exception of the stainless steel liner, do not affect susceptibility to hydrogen embrittlement at other locations:

a. Remove 1-in. nozzles by girth cuts through the vessel, and reweld the shortened vessel at two girth points (Figure No. 23).

b. Remove 1-in. nozzles and close the opening with a mechanical plug incorporating a static seal (Figure No. 24).

c. In conjunction with any one of the nozzle corrections recommended above, incorporate a thin (1/8-in. to 1/4-in. thick) austenitic stainless steel liner completely enclosing the inner surfaces of the receiver with the outer surface of the liner being vented through the wall structure to the atmosphere (Figure No. 25). This is considered the most desirable alternative.

5. Pending the availability of sufficient additional data regarding the effect of high pressure hydrogen gas upon available receiver materials, accompanied by design parameters that can be utilized with confidence, it is recommended that the austenitic stainless steel liner approach per 4.c above (Figure No. 25) be utilized for new procurement receivers for storing hydrogen gas above 3600 psi.

VI. STRUTHERS WELLS GAS RECEIVERS

A. INTRODUCTION

Three gas receivers were procured from the Struthers-Wells Corporation for the M-1 Program. These units are 1300 cu ft, 5000 psi vessels. One was intended for gaseous hydrogen service and two for nitrogen service. All were to be installed in the new K-Zone for engine testing. Only one of these receivers, VK-11, was placed in service. This was as a replacement for an A.O. Smith hydrogen receiver in H-Zone, as shown on Figure No. 26. This replacement receiver failed after 17 days of operation. Internal inspection revealed an extensive crack along a main longitudinal seam as well as other defects. Internal inspection of the two unused receivers also revealed internal defects.

B. DESCRIPTION

These receivers are 1300 cu ft water volume, 60-in. inner diameter, 71-3/4-in. outer diameter with an over-all length of 69 ft 11-in. One 8-in. discharge nozzle is centered in the hemispherical head. Two 1-in. and one 2-in. accessory nozzles are installed in the receiver shell. Access man-ways are not incorporated.

As shown on Figure No. 27, shell construction is of seven courses of 9 ft to 9 ft 4-in. lengths butt-welded together. Each course is comprised of four layers. The inner layer is 1-3/8-in. thick and successive layers are 1-3/8-in., 1-1/2-in., and 1-5/8-in. Each layer is separately rolled from plate, seam-welded into a controlled-dimension shell, and shrink-fitted over its internal adjacent layer.

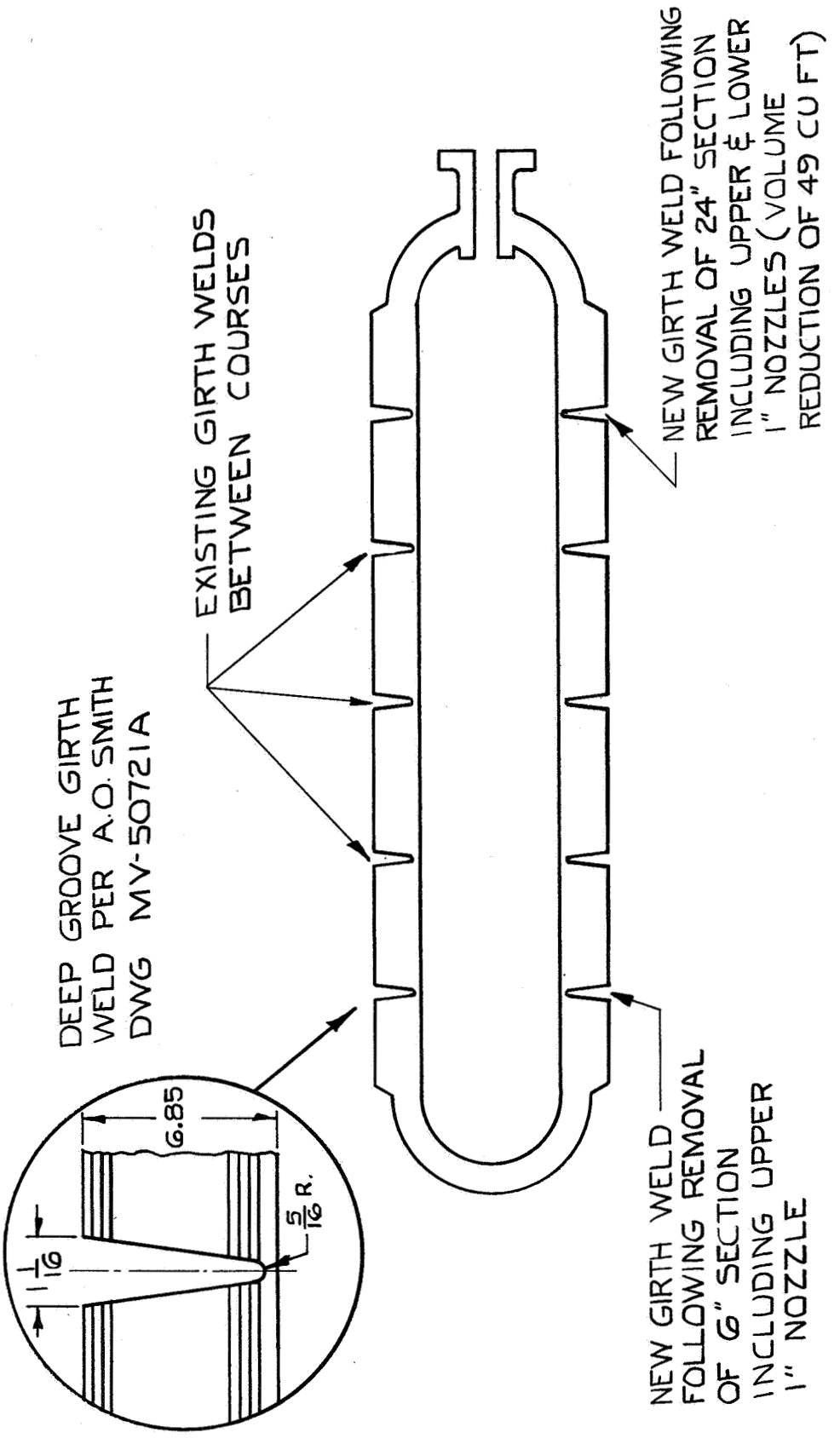

Figure 23: Proposed Section Removal and Girth Weld

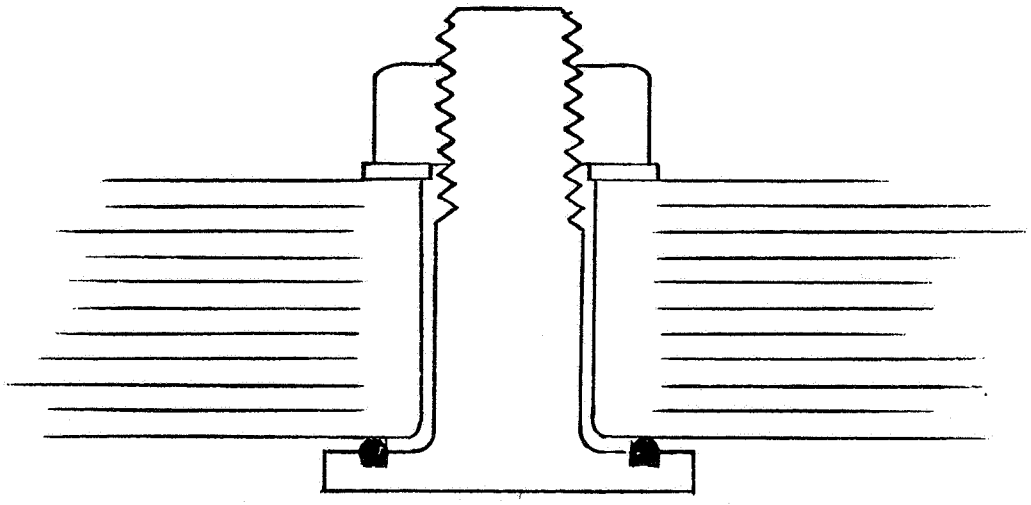

Figure 24: Tension Plug, Static Seal Replacement

ADVANTAGES

1. Relatively Economical.
2. Removes Residual Stress (Stress Riser Areas from High-Pressure Hydrogen Exposure.

DISADVANTAGES

1. Requires Static Seal at Curved Inner Surface with Doubtful Performance, or Machined Flat Surface with Discontinuity to Inner Lamination.

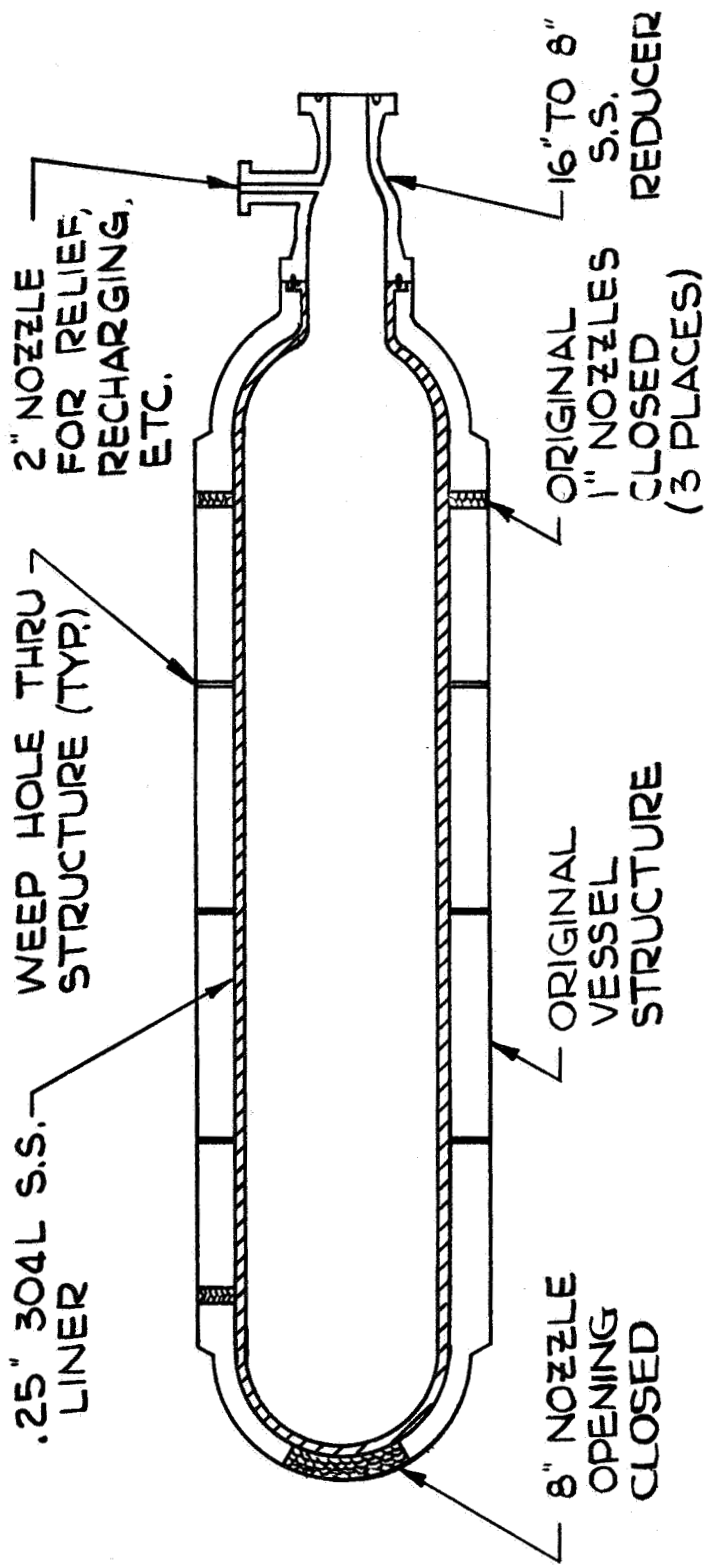

Figure 25: Proposed Liner Installation, Configuration "A": Single Nozzle

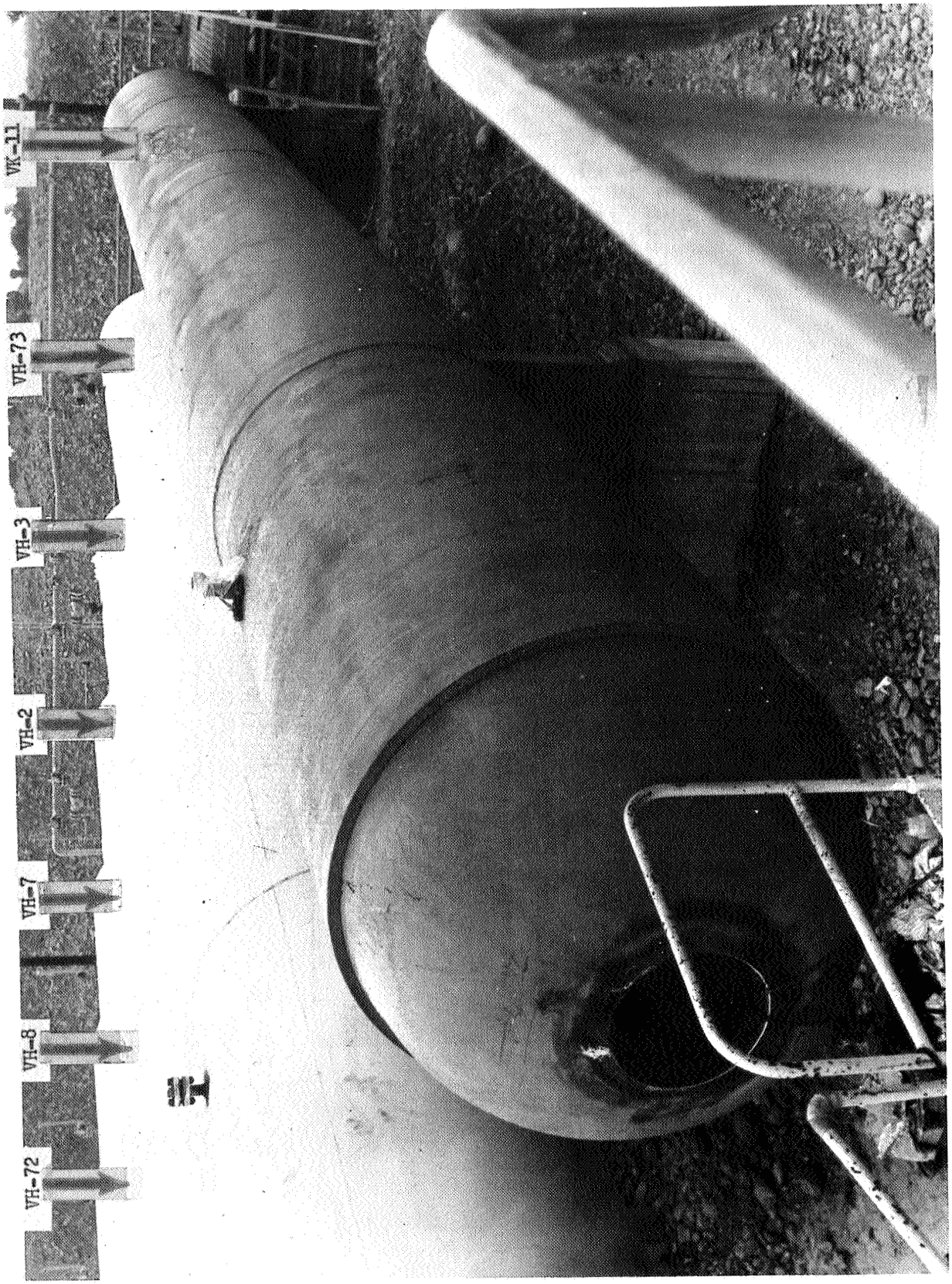

Figure 26: Receiver VK-11 Installed in H-Zone Cascade

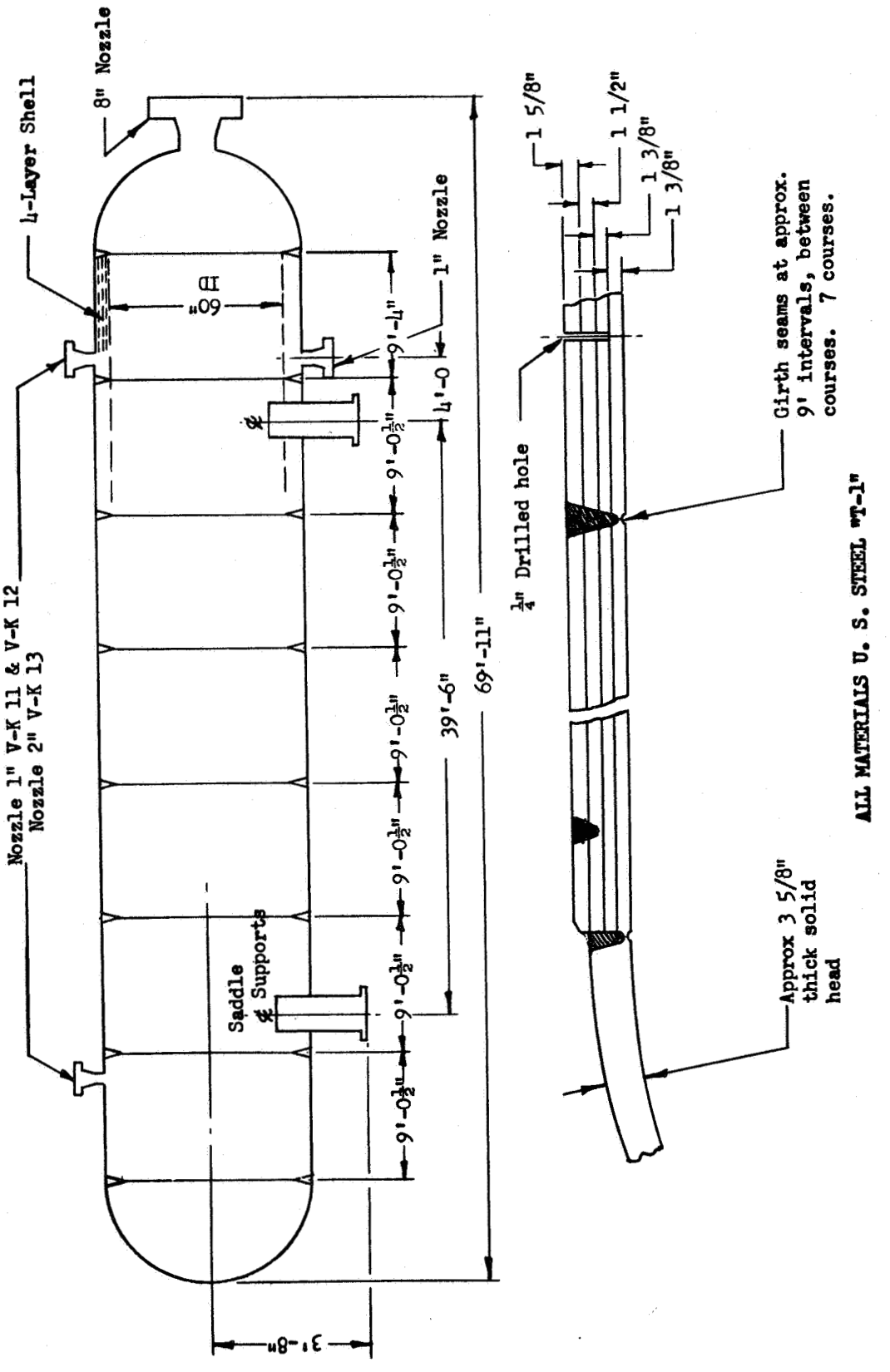

Figure 27: SWC High Pressure Receiver

All material of the receiver is U.S. Steel, "T-1" with shell plates quenched and tempered to 115,000 psi tensile yield strength; heads and nozzles are quenched and tempered to 105,000 psi tensile yield strength. The submerged arc process with SWC-APS-4-S rod and procedure is used for all seam and girth welds. Manual welding of the nozzles is with SWC-PBX-15.

The receiver was completely stress relieved after welding at 1050°F in three sections. Two final closing girth welds were induction-heated for stress relief.

Radiograph inspection was made of all girth and longitudinal seams. A hydrotest was performed to 7500 psi.

C. FAILURES AND DEFECTS

The receiver VK-11 was initially pressurized on 16 May 1965 and failed on 1 June 1965 with the 17 day operation history described on Table 5. Inspection access was obtained by cutting a 24-in. hole in the static head. As shown on Figure No. 28, a crack approximately 50-in. long was found in the Course No. 5 along the layer longitudinal weld and penetrating the complete thickness of the 1-3/8-in. thick inner layer for a portion of this length. Two smaller cracks of unknown depth also were found along the longitudinal weld in course No. 1 (see Figures No. 29 through No. 31).

Unused receivers VK-12 and VK-13 were entered for internal inspection in the same manner as VK-11. Defects found in these units are shown on Figures No. 32 through No. 34. Exploratory grinding of one crack in Course No. 5 of receiver VK-12 revealed a crack depth of approximately 1/4-in.

D. INVESTIGATION

Aerojet-General conducted a metallurgical investigation and made tensile tests of specimens cut from around the major crack in VK-11. The fracture characteristics in the heat-affected zones of both the initial and repair welds were of a nature that indicated a failure sequence of cracking during welding followed by propagation of the cracks as a result of pressurizing the vessel. The 0.2% offset yield strength of the parent material ranged from 127.0 to 131.2 ksi. The joint efficiency of the weld was about 88% based on 0.2% offset yield strength.

The Struthers-Wells Corporation has completed an exploratory X-Ray inspection of all units in an attempt to establish the condition of the outer three layers. Results of this inspection have not been made available.

Aerojet-General proposed a program for inspection of Courses 1 and 5 of Vessel VK-11 by destructive disassembly as a prerequisite to establishing repair procedures for the other receivers. Struthers-Wells indicated their desire to accomplish this inspection and VK-11 was returned to the Titusville, Pa. plant. Prior to disassembly, a complete

SERVICE AND FAILURE HISTORY
SWC RECEIVER VK-11

Date	Time		Pressure	
March 1964		Hydro-Test	0/7500/0	H_2O
5/3/65		Installation		
5/12/65		Leak Test	0/4200/0	N_2
5/16/65	0915/2200		0/3500	H_2
5/17/65	1645/1800		3123/2350	H_2
5/18/65	0940/1440		2900/3500	H_2
5/19/65	1930/0300		1200/3600	H_2
5/20/65	0450/0600		2200/2600	
5/21/65	0600/1725		2500/3500	H_2
5/22/65	Sat - No Work			
5/23/65	Sun - No Work			
5/24/65	Repairing GH_2 block valve no pumping.			
5/26/65	1100/0600		1200/2200 and 2000/3300	H_2
5/27/65	0600/0200		3100/3300 and 2100/3200	H_2
5/28/65	0600/0635		3200/3300	H_2
5/29/65	Holiday - Sat			
5/30/65	Sunday			
5/31/65	Holiday			
6/1/65	0800/1600		1250/3900	H_2
6/1/65	2100		3900 Failure	H_2

Table 5

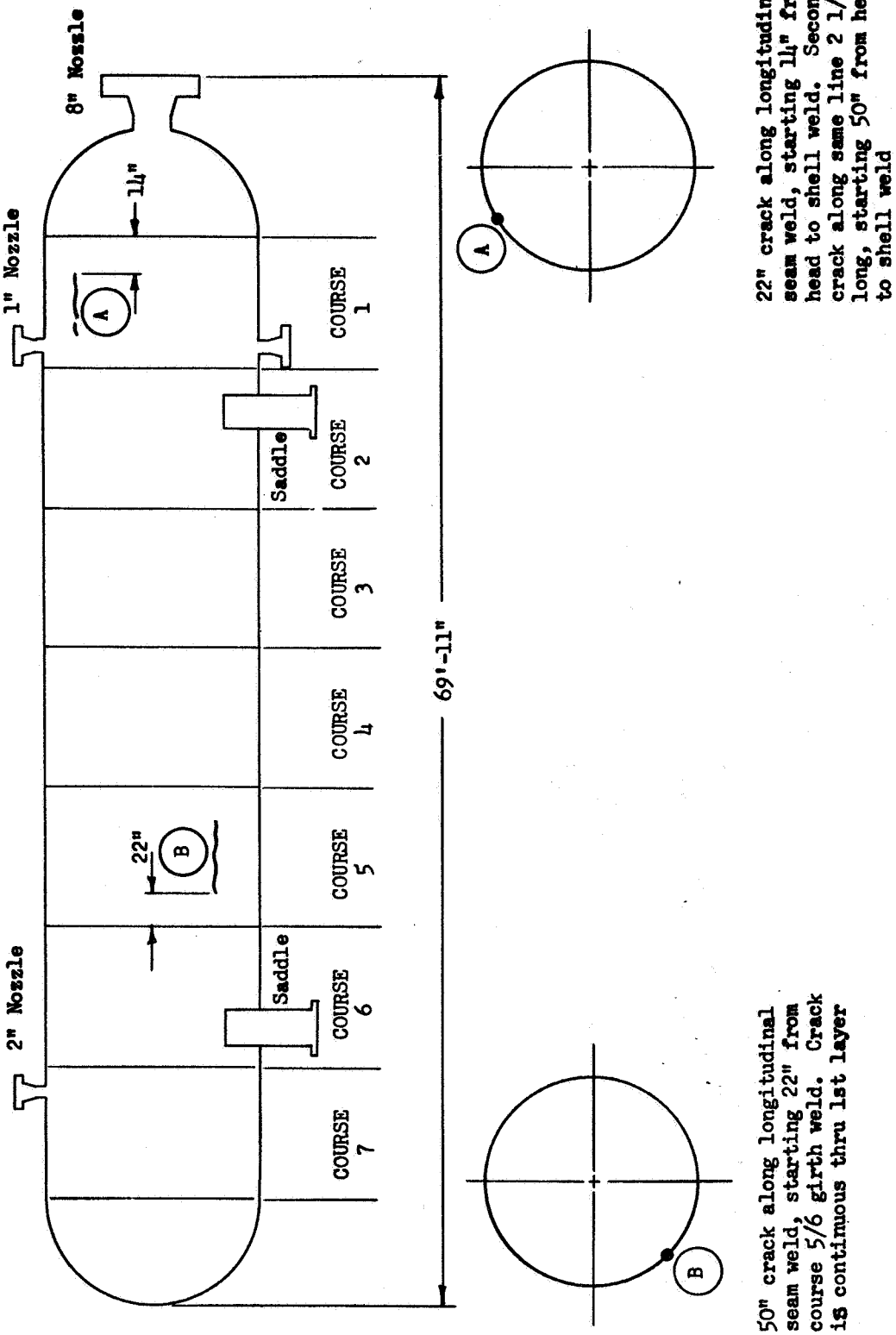

Figure 28: Receiver VK-11, Location of Failure Crack and Other Defects

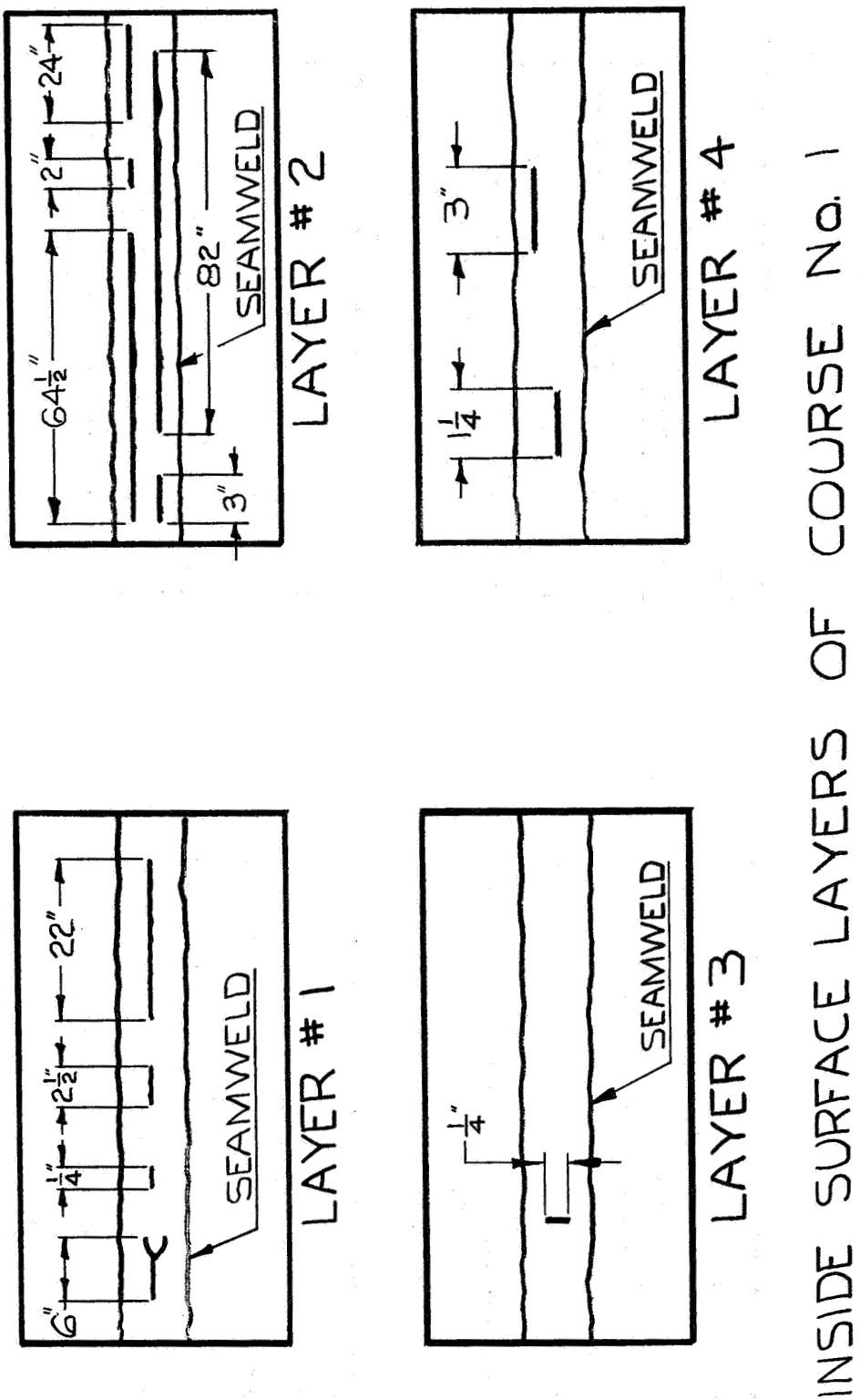

Figure 29: Receiver VK-11, Location of Cracks, All Layers of Course No. 1

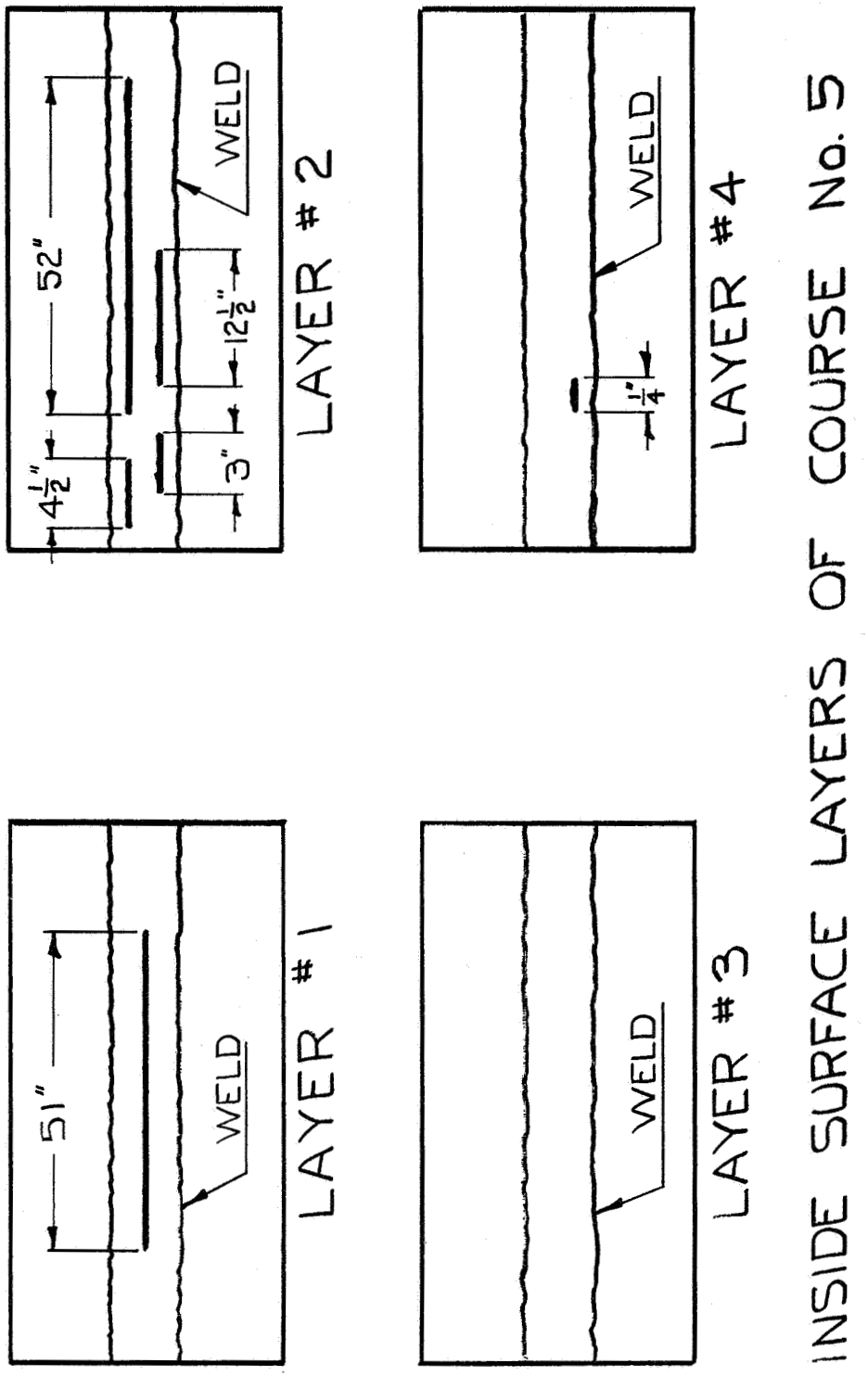

Figure 30: Receiver VK-11, Location of Cracks, All Layers of Course No. 5

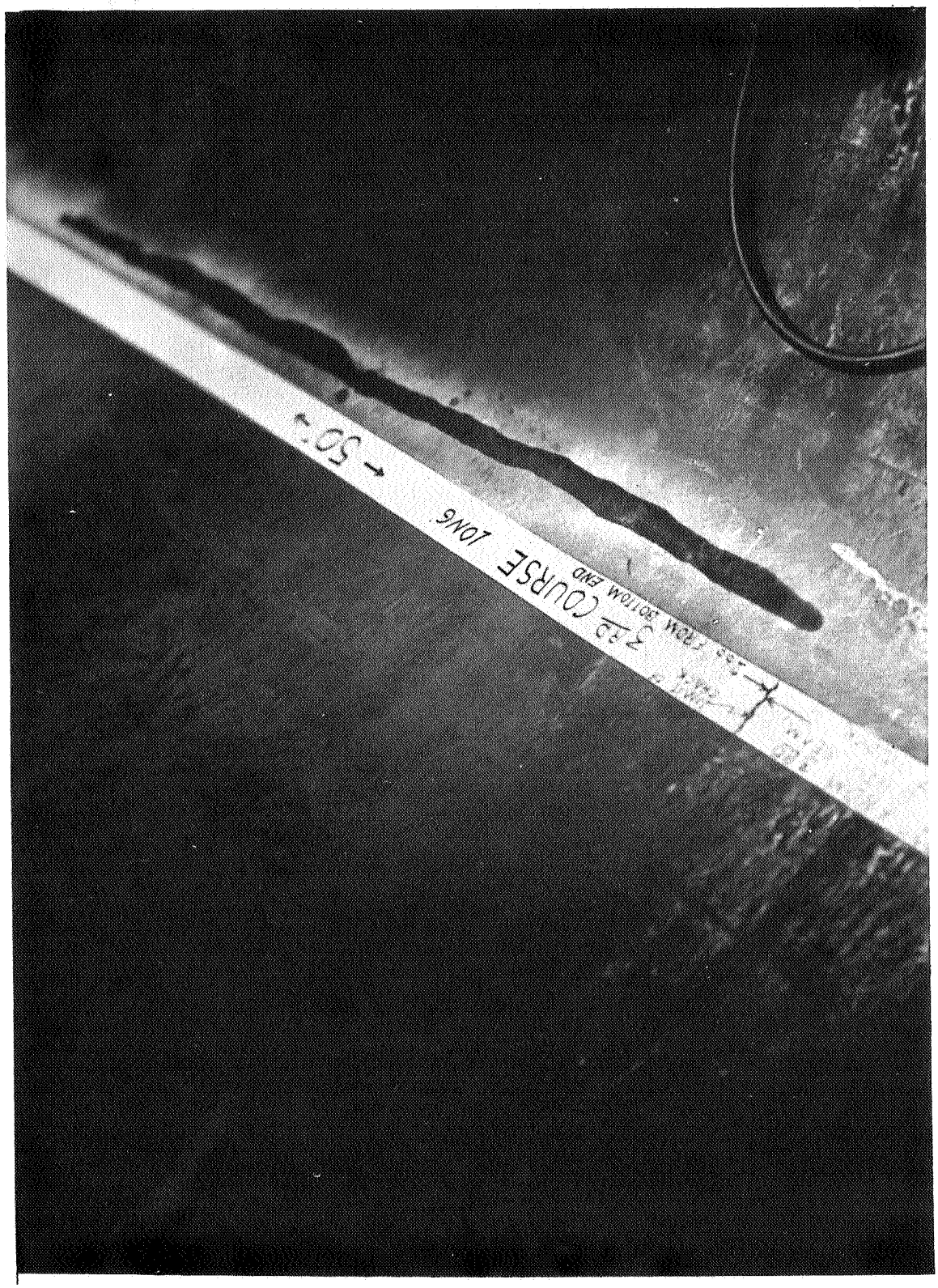

Figure 31: Receiver VK-11, Interior of Course No. 5

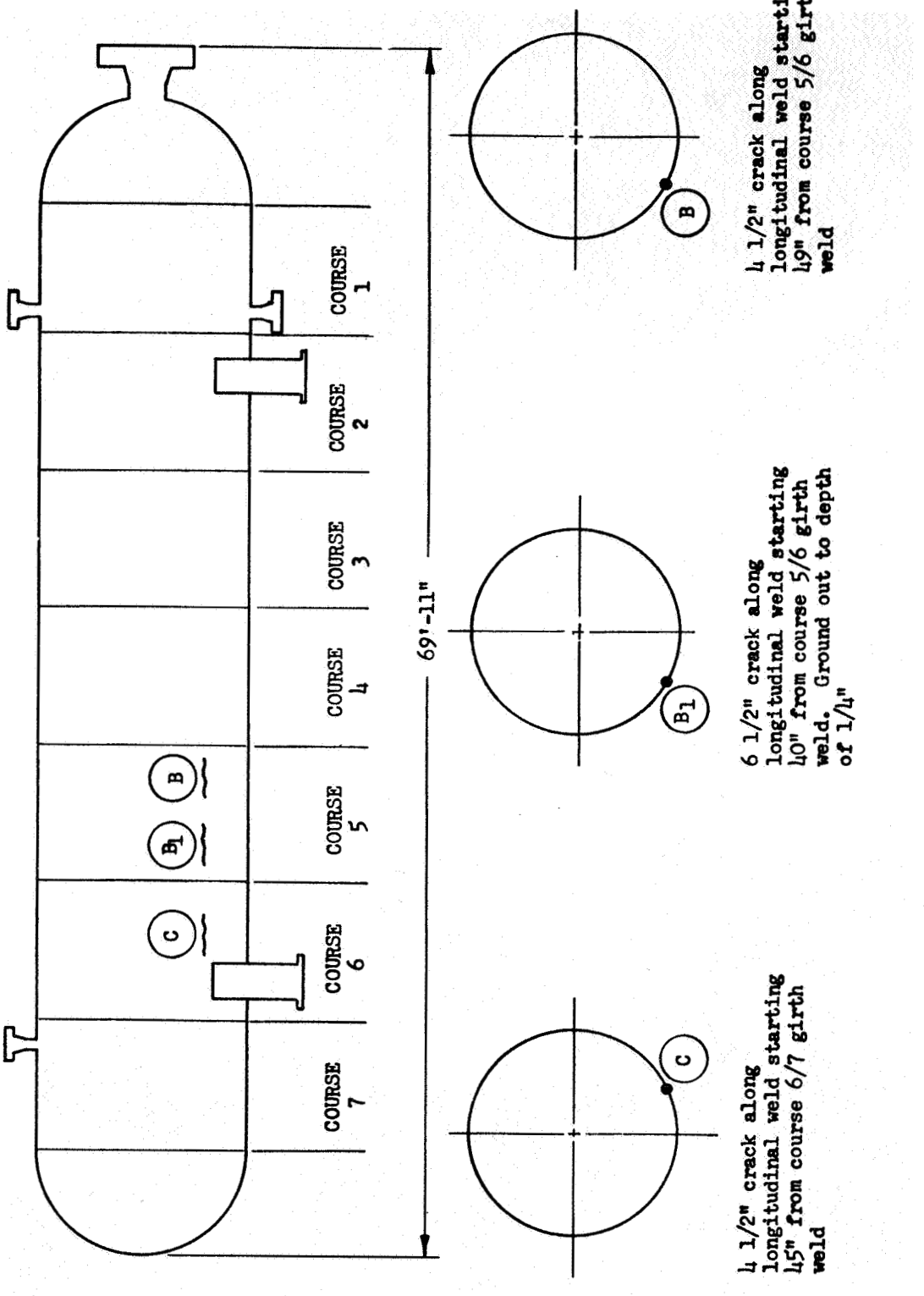

Figure 32: Receiver VK-12, Location of Defects in Inner Layer

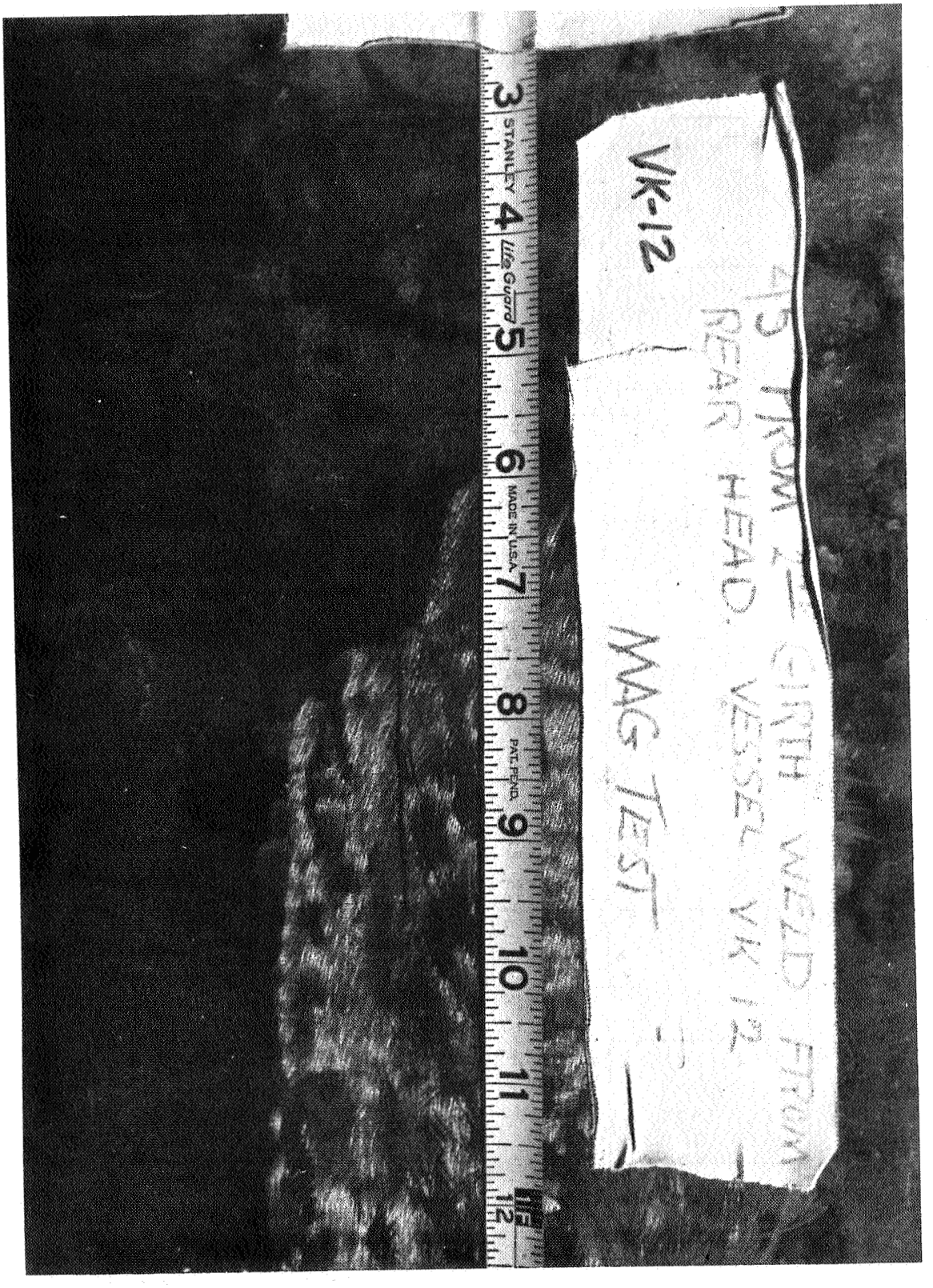

Figure 33: Receiver VK-12, Interior of Course No. 6

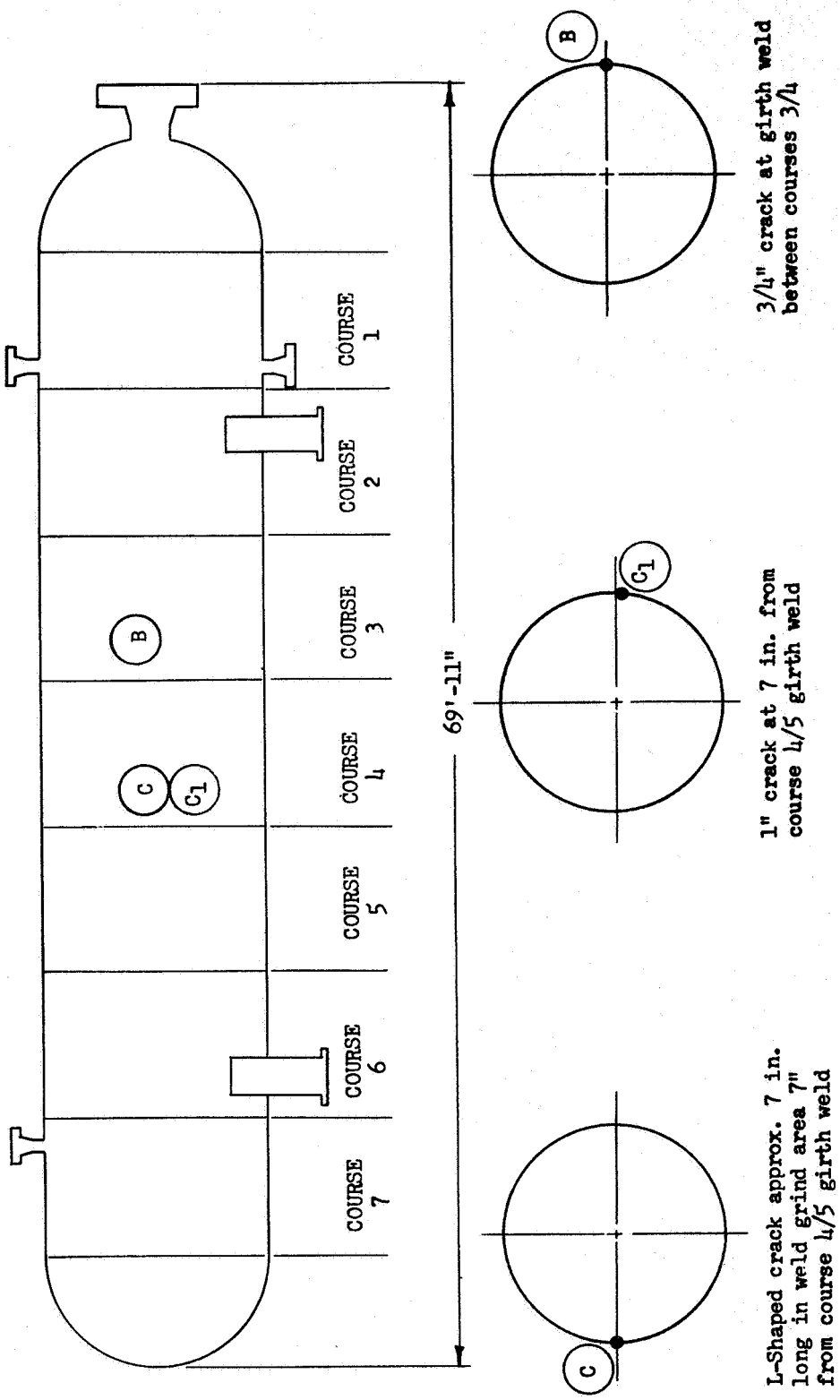

Figure 34: Receiver VK-13, Location of Defects in Inner Layer

radiographic inspection was made of Courses 1 and 5 and an approximately 50% inspection was made of the remaining courses. In addition to the known cracks, others of equal or even greater extent were disclosed. Verification of the location of these additional cracks in a particular intermediate layer was accomplished by disassembly of Courses 1 and 5. This disassembly was accomplished by slitting each successive layer and slipping it off the remaining layers. The cracks found in each layer are shown on Figures No. 29 and No. 30. A crack of at least 14 inches long in Course 2 was located by the radiographic inspection. Verification by disassembly was not attempted.

E. CONCLUDING REMARKS

1. The failure of vessel VK-11, the subsequent metallographic and radiographic inspection, and the disassembly inspection of VK-11 as well as the inner surface inspections of both VK-12 znd VK-13 indicate that vessel VK-11 was inadequate as manufactured.

2. The application of T-1 steel in high-pressure receivers is subject to the same general conclusions and recommendations as regards exposure to hydrogen gas, reviews of structural design, as well as fabrication and inspection as were presented in Sections IV and V of this report.

3. The welding and stress-relief procedures applied to T-1 steels in pressure vessels must be considered to be critical and should be subjected to precise control.

4. No practical means for repairing vessel VK-11 has been advanced. Vessels VK-12 and VK-13 are subject to the same manufacturing inadequacies and the actual condition of their interior layers is unknown. Therefore, the further utilization of these vessels appears to be inadvisable.

BIBLIOGRAPHY

1. Beachum, E.P., Johnson, H.H., and Stout, R.D., "Hydrogen and Delayed Cracking in Steel Weldments," Welding J., Research Supplement, v 40, n 4, pp 155-159, April 1961.

2. Cavett, R.H., and VanNess, H.C., "Embrittlement of Steel by High-Pressure Hydrogen Gas," Welding J., Research Supplement, v 42, n 7, pp 316s-319s, July 1961.

3. Corruccini, R.J., Hydrogen Embrittlement of Steels, Cryogenic Engineering Laboratory, National Bureau of Standards, Project No. 81131, March 1962.

4. Elsea, A.R., and Flatcher, E.E., Hydrogen-Induced, Delayed Brittle Failures of High Strength Steels, DMIC Rpt. 196, Defense Metals Information Center, January 1964.

5. Fletcher, E.E., and Elsea, A.R., "The Effects of High-Pressure, High Temperature Hydrogen on Steel," DMIC Rpt. 202, Defense Metals Information Center, March 1964

6. Hobson, J.D., and Sykes, C., "Effect of Hydrogen on the Properties of Low-Alloy Steels," J. of Iron and Steel Institute, v 168, pp 209-220, Nov 1951.

7. Hoffman, W., and Rauls, W., "Ductility of Steel Under the Influence of High Pressure Hydrogen," Welding J., Research Supplement, v 44, n 5, pp 225s-230s, May 1965

8. Hoffman, W., and Rauls, W., "New Observations on the Embrittlement of Steel by Hydrogen at Room Temperature," Dechema-Monographien NR. 734-760, pp 33-39, 1962

9. Marchall, C.W., The Factors of Influencing the Fracture Characteristics of High Strength Steel, DMIC Report 147, Defense Metals Information Center, pp 32-35, February 1961.

10. Mills, R.L., and Edeskuty, F.J., Hydrogen Embrittlement Tests of Cryogenic Metals, Los Alamos Scientific Laboratory, University of California, Los Alamos, N.S.

11. Mills, R.L., and Edeskuty, F.J., "Hydrogen Embrittlement of Cold-Worked Metals," Chem. Engr. Progress, v 52, n 11, pp 477-480, November 1956.

BIBLIOGRAPHY (Cont.)

12. Nelson, G.A., and Effinger, R.T., "Blistering and Embrittlement of Pressure Vessel Steels by Hydrogen," Welding J., Research Supplement, v 34, pp 12s-21s, January 1955

13. Perlmutter, D.D., and Dodge, B.F., "Effects of Hydrogen on Properties of Metals," Ind. and Engr. Chem, v 48, n 5, pp 885-893, May 1956

14. Aerojet-General Corp., Materials Engineering Report FA 65-179, Failure Analysis of GH_2 Pressure Vessel, 6 April 1965.

15. VanNess, H.D., and Dodge, B.F., "Effects at High Pressure on the Mechanical Properties of Metals," Chem. Engr. Progress, v 51, n 6, pp 266-271, June 1955.

NASA-Langley, 1969 —— 17 E-4774